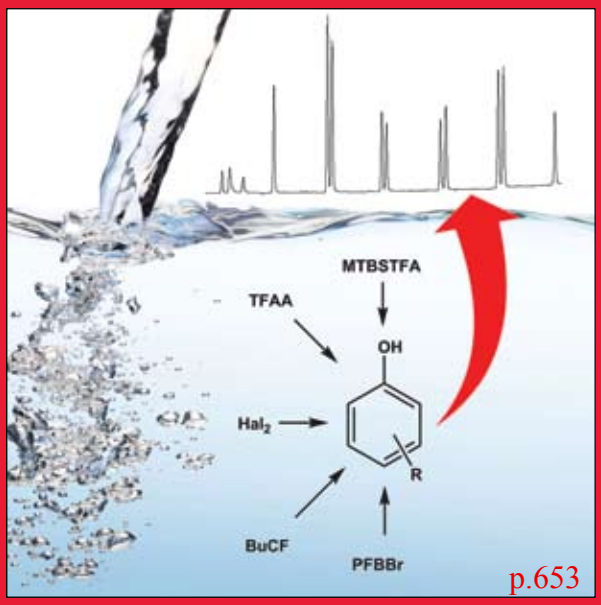
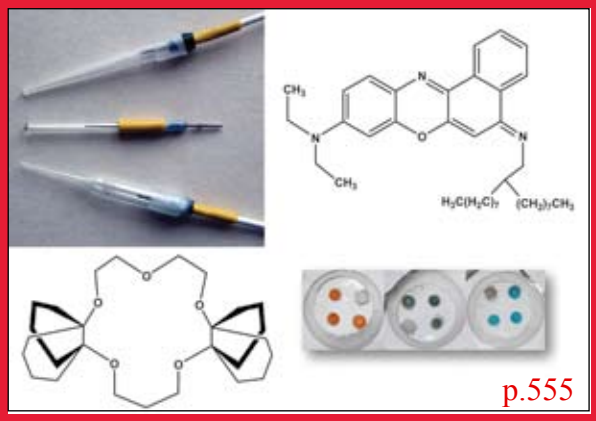
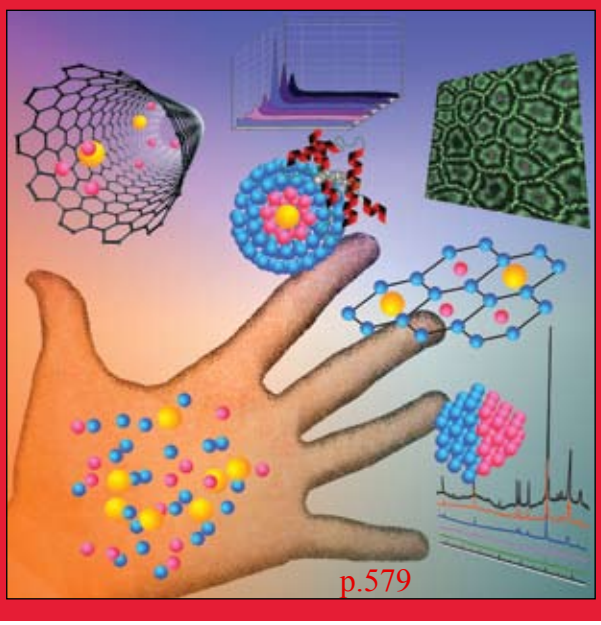
ISSN 0036-021X

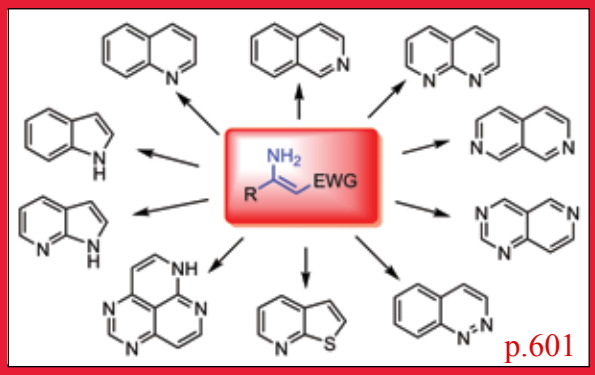
Russian Chemical Reviews



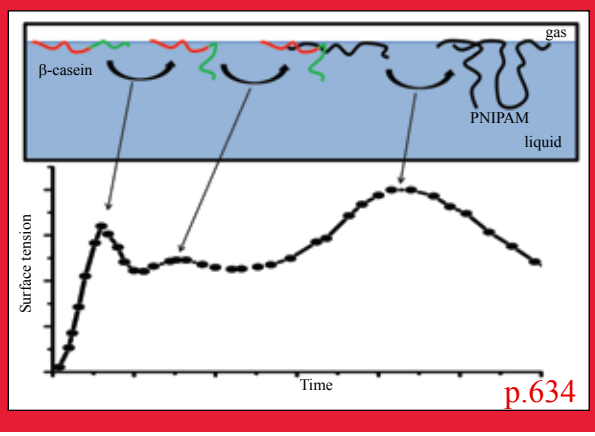
p.653


p.555


p.579



p.601



p.634

Reviews on current topics in chemistry

The Chemistry at the Saint Petersburg State University

Volume 84 2015 Number 6

Russian Chemical Reviews **84** (6) 579 – 600 (2015) © 2015 Russian Academy of Sciences and Turpion Ltd

DOI 10.1070/RCR4487

Hybrid nanostructures: synthesis, morphology and functional properties

A V Povolotskaya,[a] A V Povolotskiy,[b] A A Manshina [b]

[a] Research Park, Center for Optical and Laser Materials Research, Saint Petersburg State University ul. Ul'yanovskaya 5a, Peterhof, 198504 Saint Petersburg, Russian Federation
[b] Institute of Chemistry, Saint Petersburg State University Universitetskiy prosp. 26, Peterhof, 198504 Saint Petersburg, Russian Federation

Hybrid nanostructures representing combinations of different materials and possessing properties that are absent in separate components forming the hybrid are discussed. Particular attention is given to hybrid structures containing plasmonic and magnetic nanoparticles, methods of their synthesis and the relationship between the composition, structure and properties. The functional features of the hybrid nanomaterials of various morphology (with core – shell structures, with encapsulated metal nanoparticles and with metal nanoparticles on the surface) are considered. The unique properties of these hybrid materials are demonstrated, which are of interest for solving problems of catalysis and photocatalysis, detecting impurities in various media, *in vivo* visualization, bioanalysis, as well as for the design of optical labels and multifunctional diagnostic nanoplatforms.
The bibliography includes 182 references.

Contents

I. Introduction 579
II. Methods of synthesis 580
III. Functional properties 584
IV. Conclusion 597

I. Introduction

Unlike nanocomposites, which are usually formed upon introduction of nano-sized elements (fillers) into a solid matrix, hybrid nanomaterials are combinations of nanostructures differing in the composition and type: nanoparticles, nanotubes, nanofibres, nanoplates and so on. Hybrid nanomaterials contain nano-sized components and the overall size of the hybrid material is, most often, also in the nanometre range. From the standpoint of morphology, hybrid nanomaterials are classified into core – shell structures;[1–6] Janus type nanostructures combining two (or more) components with similar size;[7–9] and nanostructures (nanoparticles, nanotubes or nanoplates) containing nanocomponents that are either encapsulated or deposited on the surface.[10–13]

The interest in these materials inhomogeneous in the composition and structure is determined by the properties acquired by a hybrid nanomaterial due to association of the initial nanocomponents. Furthermore, combination of different components in the same structure not only sums up the properties of separate components but, in some cases, endows the hybrid structure with new properties due to the synergistic effect. An example is provided by enhancement of luminescence upon combination of luminescent nanoparticles (quantum dots, nanoparticles with lanthanide ions) with metal nanoparticles exhibiting surface plasmon resonance. By varying the component set, ratio, composition, size, shape and structure, it is possible to design hybrid materials with a broad range of functional properties.

The studies carried out to date demonstrated that hybrid nanomaterials are essential for biology and medicine, sensor technology, green chemistry and other fields.[14–16] In addition, design of hybrid systems not only offered materials with desired functional properties but was also beneficial for the advent of new potent analytical methods suitable for solving problems of detection and identification of impur-

A V Povolotskaya Candidate of Physical and Mathematical Sciences, Deputy Director of the RP COLMR SPbSU.
Telephone: +7(812)324 – 1270, ext. 5824,
e-mail: anastasia.povolotckaia@spbu.ru
A V Povolotskiy Candidate of Physical and Mathematical Sciences, Associate Professor at the Chair of Laser Chemistry and Laser Material Science of the Institute of Chemistry SPbSU.
Telephone: +7(812)428 – 4335, e-mail: alexey.povolotskiy@spbu.ru
A A Manshina Candidate of Physical and Mathematical Sciences, Associate Professor at the same Chair.
Telephone: +7(812)428 – 4335, e-mail: manshina@chem.spbu.ru
Current research interests of the authors: laser chemistry, laser physics, solid state chemistry, nanostructured materials, optical spectroscopy.

Received 14 August 2014
Uspekhi Khimii **84** (6) 579 – 600 (2015); translated by Z P Svitanko

ities, substance preconcentration and separation and *in vivo* visualization and targeting.[17–19]

Analysis of publications devoted to hybrid materials demonstrated that the scope of their application is most often specified by the properties of one of the components. Additional components either extend the functional properties in the same area or increase the overall system efficiency. For instance, nanostructures with magnetic nanoparticles can be controlled by an external magnetic field; they are used as contrast agents in magnetic resonance imaging (MRI) or for targeted drug delivery. Hybrid materials based on magnetic nanoparticles with addition of luminescent nanostructures can serve to visualize the site of delivery.

Special properties of hybrid nanomaterials dictate the persistent interest of researchers in preparing and studying them and, hence, publication of a rather large number of reviews dealing with analysis and systematic account of the properties of such materials.[20–24]

The present review covers the functional properties and considers the possible applications of hybrid nanostructures. Primary attention is given to preparation methods and properties of hybrid nanostructures containing plasmonic and magnetic nanoparticles as key components determining the functions and the scope of application of nanohybrids. The presence of magnetic components provides the function of directed motion and spatial control of hybrid nanomaterials. Owing to plasmonic properties, there is the possibility of enhancing luminescence and Raman signals. By combining magnetic and/or plasmonic nanostructures with other nanocomponents, it is possible to extend the range of properties with maintenance of functions set by the major component. The review analyzes the data on the indicated subject published in the last $\sim$10 years.

II. Methods of synthesis

Three fundamentally different approaches to the synthesis of hybrid nanostructures have been formed to date: aggregation[10,11] and sequential[1–8] and parallel syntheses.[12,13] The first approach implies the formation of nanoparticles and their further aggregation to form a single structure. Actually, this approach is a development of the 'bottom-up' synthetic strategy which does not stop after the formation of single nanoparticles/nanostructures but also includes the subsequent formation of complex multicomponent materials upon aggregation of the initial nanostructures to give the final hybrid.

The most popular second approach includes a sequence of reactions, resulting in multilayer film structures, nanoparticles in the matrix pores or core–shell nanostructures. The third approach implies parallel synthesis of hybrid nanostructures and nanoparticles that form the hybrid, without pretreatment of components.

II.1. Synthesis of nanostructures by aggregation

The synthesis of nanostructures by aggregation starts with the formation of nanoparticles, which are subsequently aggregated into a single structure.[10,11] Quite a number of publications are devoted to the synthesis of nanoparticles by various methods. Most popular are 'wet chemistry' methods, lithography, plasma-chemical deposition, laser ablation and laser deposition.[25–28] The obtained nanoparticles can be assembled into a single structure in various combinations and proportions. This gives hybrid nanostructures that not only combine the properties of constituent nanoparticles but often also possess new unique properties, which arise, first of all, due to the large interfacial area between the components of the hybrid structure.[20]

The synthesis of hybrid nanostructures according to the aggregation principle[10,11] is not widely used as yet. This is caused by the difficulty of obtaining a homogeneous distribution of nanoparticles of various compositions in the hybrid structure. Nevertheless, laser methods based on the thermal (photothermal) mechanism of formation of hybrid structures from nanoparticles are used fairly successfully.[29,30]

The thermal mechanism of laser-induced aggregation is based on the principle of melting and association of nanoparticles in the colloid solution.[29,30] Laser methods can be used for the formation of hybrid nanostructures of a complex shape.[10] If a photon flux of laser radiation serves as the source of energy for heating nanoparticles, the mechanism is called photothermal. Bahns *et al.*[10] synthesized hybrid nanostructures in an aqueous colloid solution of gold and carbon (Fig. 1). The synthesis was carried out in a solution drop under continuous irradiation with an argon laser (wavelength λ = 488 nm, power W = 1 mW and focal spot area of 0.3 μm^2). The obtained structures consisted of gold and carbon nanoparticles. By moving the focused laser beam in a colloid solution, it is possible to obtain filaments — aggregates of nanostructures reproducing the focal spot trajectory, *i.e.*, hybrid nanostructures of a complex architecture can be fabricated.

The photothermal mechanism can form the basis of the laser method for aggregation of carbon nanotubes and metal nanoparticles into a single structure. Henley *et al.*[11] demonstrated the possibility of attachment of metal nano-

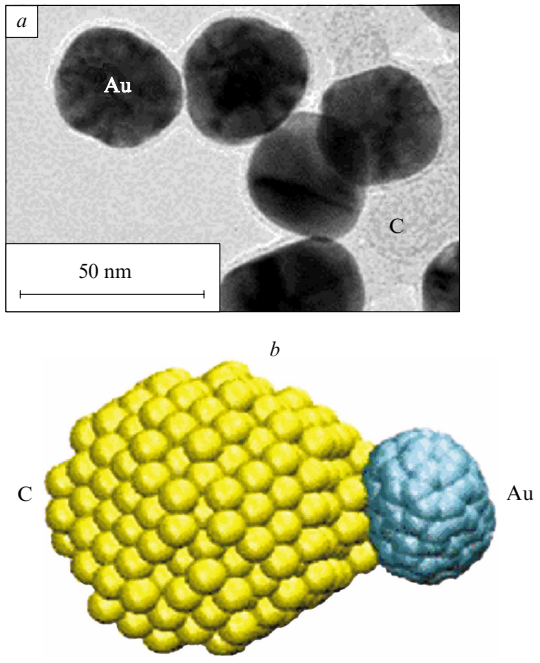


Figure 1. Transmission electron microscopy (TEM) image (*a*) and the model of hybrid nanostructure composed of gold and carbon (*b*).[10]

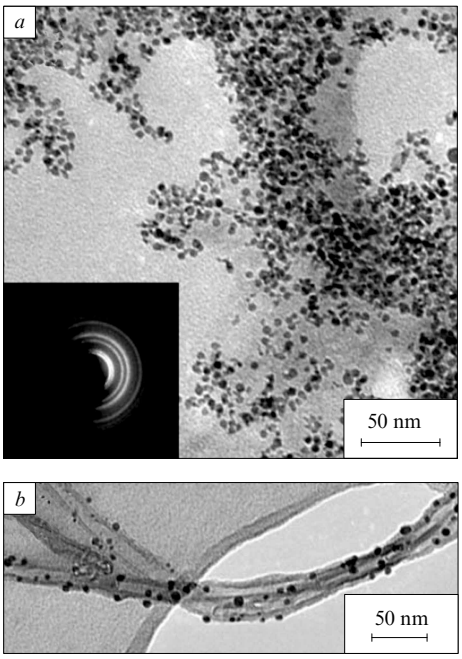


Figure 2. TEM images of Pd nanoparticles (*a*) (the inset shows the electron dispersion indicative of the crystal structure) and a carbon nanotube decorated with Pd nanoparticles (*b*).[11]

particles to nanotubes (Fig. 2) from aqueous solution on exposure to the excimer laser radiation (λ = 248 nm, pulse duration of 25 ns and fluence of 3 J cm^{-2}). Laser radiation induces the following processes: melting of colloid Pd or Au nanoparticles, decrease in their size due to boiling effect and attachment of remaining nanoparticles to the surface of carbon nanotubes.

II.2. Sequential synthesis of hybrid nanostructures

In the sequential synthesis of hybrid nanostructures, the first stage is the preparation of nanoparticles that would act as nuclei, or the matrix for the subsequent synthesis of materials. A method for the formation of gold nanoparticles on the ends of CdS nanorods (Fig. 3) was proposed.[7,8] Samples of hybrid nanostructures can be assigned to the Janus type. The average size of the CdS rods was 5.3 × 14 nm and the diameter of gold nanoparticles was ~6 nm. The CdS nanorods were grown on seeds. Gold nanoparticles were obtained by photoinduced synthesis from solution. First, a small gold island serving as the nucleus is formed on one end of the rod. Under the action of light, charge separation between the metal (Au) and the semiconductor (CdS) takes place, the electrons being concentrated on the gold nuclei. Gold cations are actively reduced on the negatively charged island, giving rise to unsymmetrical Janus hybrid nanostructures.

Shaviv *et al*.[8] carried out the experiment in the following way: a solution containing 3 ml of toluene + 20 mg of dodecylamine + 12.5 mg of dododecyldimethylammonium bromide + 8 mg of $AuCl_3$ was kept in an ultrasonic bath (15 min) and in an argon flow (3 min) and then added to a colloid solution of CdS nanorods in toluene, the mixture was stirred by an argon flux (3 min) and irradiated with a continuous laser beam (λ = 473 nm, W = 40 mW). The

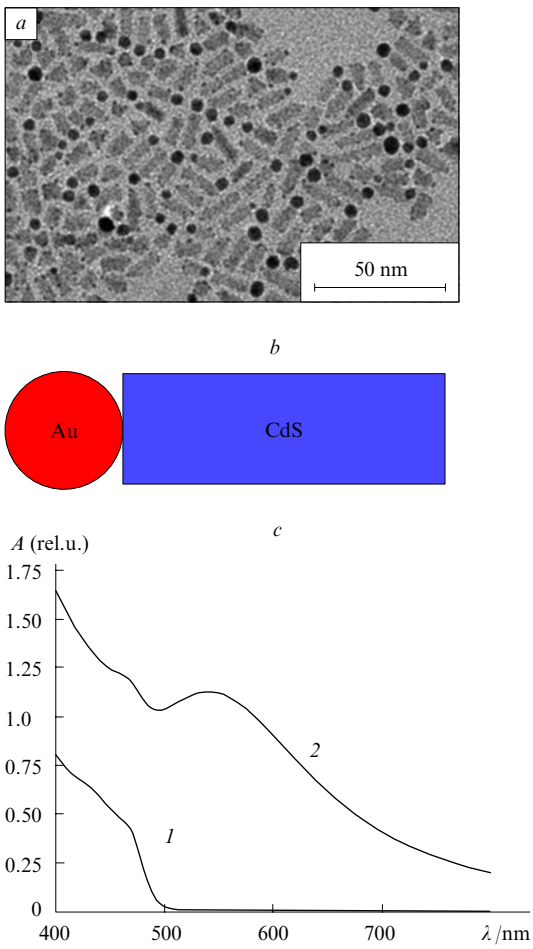


Figure 3. TEM image (*a*), scheme of CdS–Au hybrid nanostructures (*b*) and absorption spectra of CdS nanorods (*1*) and CdS–Au hybrid nanostructures (*2*) (*c*).[8]

growth of gold nanoparticles in the solution was terminated upon addition of acetone.

The photoinduced synthesis technique can be used for the formation of nanoparticles throughout the whole surface of nanorods. Berr *et al*.[31] demonstrated the possibility of decorating CdS nanorods with platinum nanoparticles.

II.2.a. Core–shell nanostructures with the metal core

Core–shell type nanostructures (an example is shown in Fig. 4) can be fabricated in various core and shell combinations depending on the type of the material: dielectric, semiconductor or metal. The selected material considerably affects the method used for the hybrid synthesis. For structures with a metal core, gold,[1,2] silver[3–5] and cobalt[6] are used most often. In this case, the shell is usually formed from a dielectric material stabilizing the metal nanoparticles.

Metal nanoparticles can be coated with a shell made of various compounds, of which SiO_2 is most popular.[1,3] Gold nanoparticles cannot be directly coated with silicon dioxide as the chemical affinity between them is weak; therefore, the surface of Au nanoparticles is pre-modified by molecules of amphiphilic non-ionic polyvinylpyrrolidone.[1] Having used the Stober process based on hydrolysis of tetraethoxysilane, for example, in aqueous ethanol with addition of ammonia

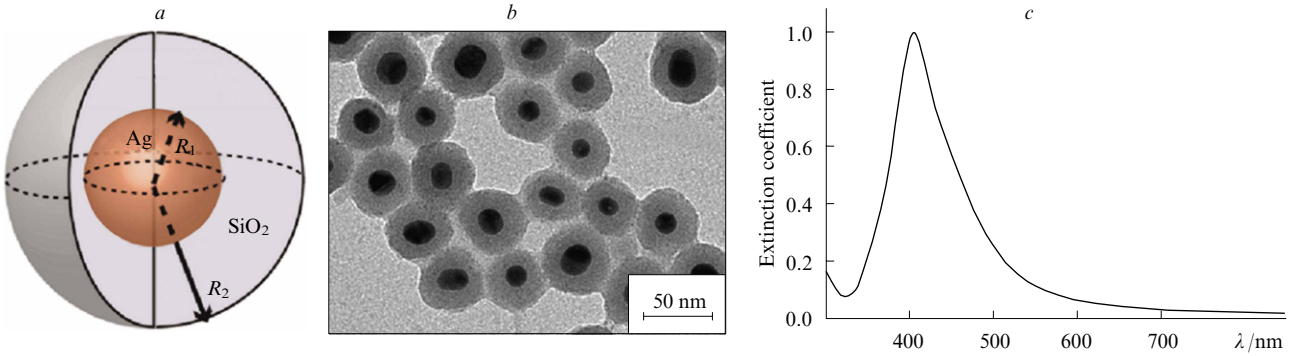


Figure 4. Scheme of core–shell nanostructure with the Ag core of the radius R_1 and the SiO_2 shell of the radius R_2 (*a*), TEM image (*b*) and absorption spectrum of such structures.[3]

as a catalyst, the authors synthesized gold nanoparticles coated with a 4 to 25 nm-thick SiO_2 shell.

Apart from the Stober method, the SiO_2 shells of metal nanoparticles can be formed by the citrate method (Turkevich method[32]) using an aqueous solution of trisodium citrate where the citrate ion serves as the reducing agent. Heating of the solution results in oxidation of the citrate ion to give acetonedicarboxylic and itaconic acids. The acids act as stabilizing agents, as they can be adsorbed on the surface of metal nanoparticle and thus restrict the nanoparticle growth. The preparation of SiO_2-coated Ag nanoparticles by the citrate method in a solution of tetraethyl orthosilicate and dimethylamine (the latter was added to produce pH in the range of 8 to 9) in ethanol over a period of 5 h has been reported.[3] Then the hybrid nanoparticles were purified by several cycles of successive washing with ethanol, dispersed in an ultrasonic bath and centrifuged (2000 rpm, 15 min).

The shells of metal core nanoparticles can consist of metal oxides, for example, Cu_2O,[2] ZnO,[6] carbon[5,33] and other substances. As a rule, the metal oxide shells are synthesized by wet chemistry techniques. For coating gold nanoparticles by a Cu_2O shell, 50 ml of an aqueous solution of $Cu(NO_3)_2$ (in a concentration of 0.01 mol litre^{-1}) containing 1 g of polyvinylpyrrolidone was used,[2] and a colloid solution of gold nanoparticles and 17 μl of a solution of $N_2H_4 \cdot 3H_2O$ (35 mass %) were added; the shells were formed for 2 min with continuous stirring. The following procedure for ZnO coating of cobalt nanoparticles was reported:[6] 0.05 mol of $CoCl_2 \cdot 6H_2O$ and 0.075 mol of citric acid monohydrate were dissolved in 100 ml of ethanol with continuous stirring at 60 °C during 6 h; $Zn(NO_3)_2 \cdot 6H_2O$ was added to the solution and stirring was continued for additional 2 h; ethanol was evaporated at 80 °C; the residue was annealed at 350 °C for 3 h; and the resulting xerogel was reduced in a hydrogen atmosphere at 450 °C for 4 h.

Silver nanoparticles in a carbon shell can be synthesized by the hydrothermal method. This method is based on the fact that at high pressure and temperature, water can dissolve compounds that are virtually insoluble under ambient conditions. The formation of Ag–C hybrid nanoparticles using a solution of 4 g of glucose and 0.1 g of polyvinylpyrrolidone in 35 ml of water containing 0.5 ml of 0.1 M $AgNO_3$ was reported;[5,30] the solution was kept in an autoclave for 4 h at 180 °C and then centrifuged and washed with deionized water, ethanol and ethylene glycol monomethyl ether.

II.2.b. Core–shell nanostructures with the metal shell

A challenging problem faced by the synthesis of hybrid nanostructures is to provide stability of a shell to corrosive environments; therefore, noble metals, in particular, gold, are used most often to form the shells. Gold immobilization on the surface was reported.[34,35] Oldenburg *et al.*[34] described the design of the SiO_2–Au (core–shell) nanostructures. 3-Aminopropyltriethoxysilane molecules were adsorbed on SiO_2 nanoparticles to completely coat the surface. Then a colloid solution containing gold particles 1–2 nm in diameter was added, and covalent bonds were formed between gold and the organosilane molecules *via* amino groups. The structures obtained in this way — gold nanoparticles deposited on the SiO_2 surface — can function as crystallization centres. When SiO_2 particles are placed into a mixture of hydrogen tetrachloroaurate(III) with potassium carbonate and a sodium borohydride solution, gold is reduced to give a continuous Au shell. A similar procedure was used by Lyon *et al.*[35] to prepare Fe_2O_3–Au (core–shell) structures. The gold shell was formed upon reduction of $AuCl_4^-$ ions with formaldehyde in an aqueous solution at room temperature for 5–10 min.

II.3. Parallel synthesis of hybrid nanostructures

In the parallel synthesis of hybrid nanostructures, the formation of nanoparticles of components and the formation of the hybrid material consisting of these nanoparticles proceed simultaneously.

Wang *et al.*[36] synthesized hybrid heterophase ZnO–Au nanostructures (Fig. 5) by reduction from a non-aqueous nanoemulsion containing gold acetate and zinc acetylacetonate. Hexadecane-1,2-diol was used as the reducing agent. The synthesis was carried out upon quick heating to 280 °C and maintenance at this temperature for 15 min. It can be seen (see Fig. 5 *b*,*c*) that the hybrid structures consist of gold nanocrystals with the (200) and (111) crystallographic planes and ZnO with the (101) planes and that a common hybrid nanostructure is formed from cubic Au nanocrystallites and the hexagonal wurtzite type ZnO.

A special group is composed of laser methods of parallel synthesis of hybrid nanostructures in which the precursor containing all necessary components of the future material is subjected to laser radiation.[12,13] Nanostructures are formed upon dissociation or transformation of the precursor under the action of the laser beam; therefore, by varying parameters of laser radiation and the properties of the initial organometallic complex, it is possible to control the

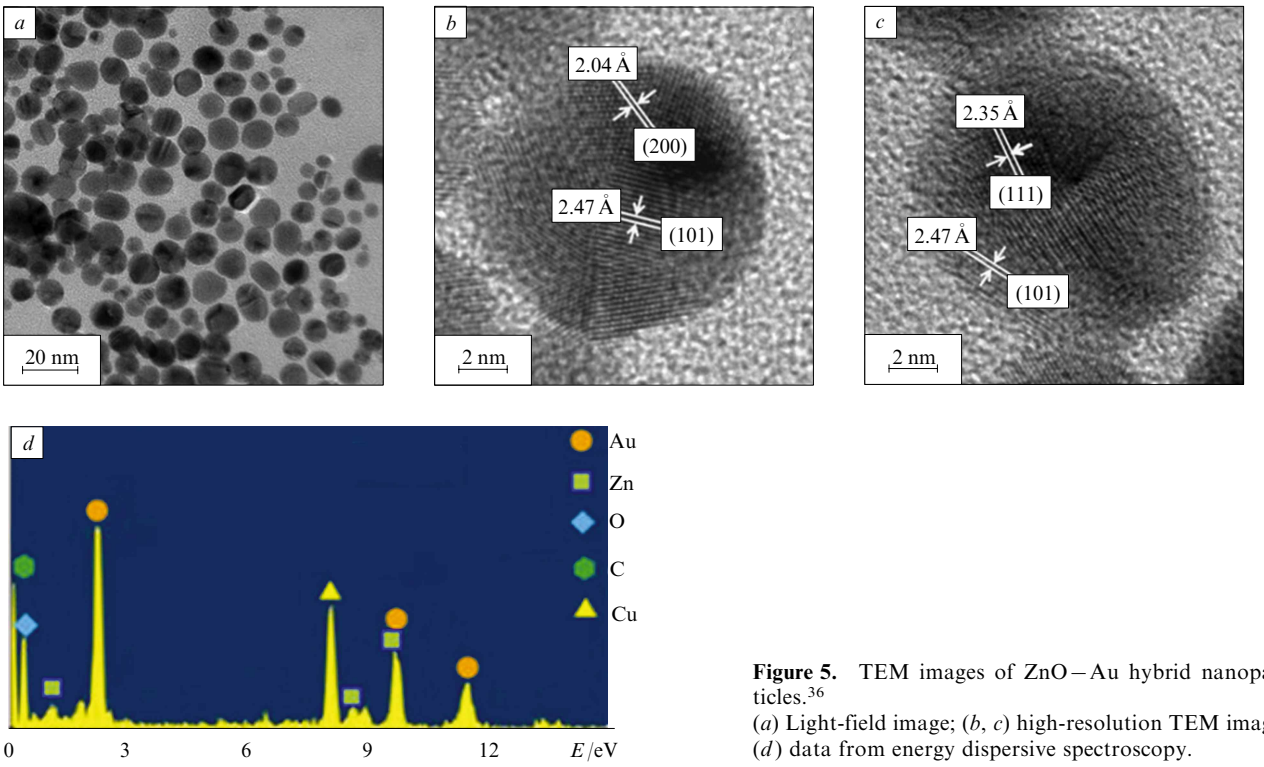


Figure 5. TEM images of ZnO–Au hybrid nanoparticles.[36]
(*a*) Light-field image; (*b*, *c*) high-resolution TEM image; (*d*) data from energy dispersive spectroscopy.

properties of the obtained nanostructures. Therefore, the precursor should meet the following key requirements: it should contain all necessary chemical components and possess light sensitivity (transition to the excited state upon photon absorption followed by a change in the structure or physicochemical properties). These requirements are met by alkynylphosphinic metal-organic complexes. For example, Koshevoy *et al.*[37] performed the laser synthesis of hybrid nanostructures using the complex $\{Au_{13}Ag_{12}(C_2Ph)_{20}[PPh_2(C_6H_4)_3PPh_2]_3\}[PF_6]_5$ (Fig. 6).

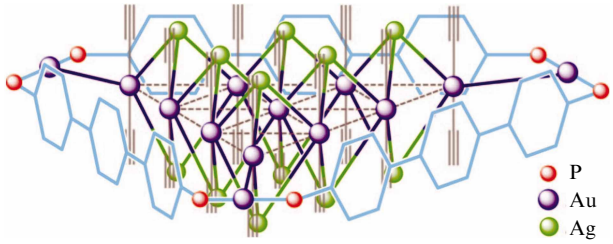


Figure 6. Schematic view of the structure of $[Au_{13}Ag_{12}(C_2Ph)_{20}(PPh_2(C_6H_4)_3PPh_2)_3][PF_6]_5$.[37]

The laser excitation of the precursor was accomplished by a continuous-wave helium cadmium laser at 325 nm, because the most intense absorption band occurs in this spectral region. The synthesis was performed in a solution of metal-organic complexes in 1,2-dichloroethane, as the complex does not dissociate in this solvent and it is transparent at the laser radiation wavelength.

A TEM image of the hybrid nanostructure is shown in Fig. 7. The presence of electron diffraction implies that the sample is partially or fully crystalline. It is noteworthy that

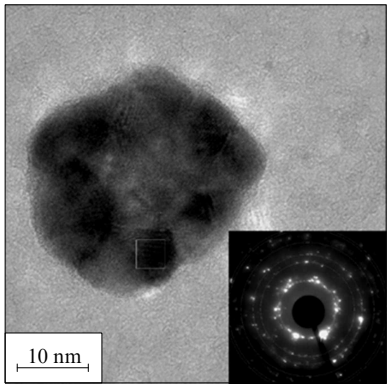


Figure 7. TEM image of the C–Au–Ag nanostructure.[13]
The inset shows the electron diffraction pattern of the obtained structure.

the non-uniform contrast of the 30-nanometre particle indicates that the structure contains at least six spherical crystalline regions.

Thus, the obtained nanostructures are hybrids consisting of two phases — carbon and metal ones. The dimensions of the carbon matrix determine the total size of the structure (20–300 nm), which incorporates metal (gold, silver) nanoclusters of 2–5 nm size.

The information on the morphology, composition and methods of synthesis of hybrid nanostructures is summarized in Table 1. Most developed are methods for successive synthesis of core–shell type structures with the metal core or shell. If the initial nanoparticles are not coated with the second phase during the sequential synthesis, the formation of Janus hybrid nanostructures is possible. A similar sit-

Table 1. Methods for the synthesis of hybrid nanostructures of various composition and morphology.

Type of hybrid nanostructure	Designation	Method of synthesis
Heterophase	Au–C, ZnO–Au	parallel synthesis (chemical reduction); aggregation method (laser heating)
Core–shell with the metal core	Ag@SiO_2, Au@SiO_2, Co@ZnO, Au@Cu_2O, Ag@C	sequential synthesis [Stober method, Turkevich (citrate) method, hydrothermal method, chemical reduction]
Core–shell with the metal shell	SiO_2@Au, Fe_2O_3@Au	sequential synthesis (surface immobilization, chemical reduction)
Janus type	CdS–Au, CdSe–Au	sequential synthesis (photoinduced charge separation, chemical reduction)
Metal nanoparticles in a matrix	Au–Ag–C, Ag–polymer, Au–Al_2O_3, Ag–Si	sequential synthesis (photodissociation, aqueous suspension polymerization, chemical reduction, hydrothermal method)
Nanorods/nanofibres decorated with metal nanoparticles	C (nanofibres)–Au, C (nanofibres)–Pd	sequential synthesis (laser heating)

uation is possible in the synthesis of hybrid nanostructures comprising both nanorods and nanowires. Due to a large surface area, these objects virtually cannot be coated with a continuous shell; as a rule, their surface is decorated by metal nanoparticles. One more example of sequential synthesis is the formation of nanoparticles in the pores of the matrix. The methods of aggregation and parallel synthesis, which can be employed for the preparation of heterophase hybrid nanostructures, are developed to the least extent. A specific feature of the aggregation method is a combination of ready nanoparticles into a single material. During the parallel synthesis, both the nanoparticles of various phases and the hybrid nanostructure are formed simultaneously from precursors containing all necessary components.

III. Functional properties

III.1. Plasmonic hybrid nanostructures

III.1.a. Surface-enhanced Raman scattering

Currently, the surface-enhanced Raman scattering (SERS) is one of the most sensitive and effective methods for detecting very low concentrations of substances.[38–42] It is implemented, most often, using noble metal nanoparticles or specially designed substrates exhibiting the surface plasmon resonance. Upon excitation of the sample contacting with a surface coated with silver, gold or platinum nanoparticles by laser radiation at the appropriate wavelength, the intensity of the Raman spectra of the adsorbed molecules increases $\sim 10^{14}$-fold.[43–45]

The success of implementation of the SERS method largely depends on interaction between the adsorbed molecules and the surface of plasmonic nanostructures. The classical materials for SERS are metal nanostructures with a size of 1 to 100 nm. Often, metals such as gold, silver and copper are used as substrate materials for SERS; gold and silver serve most frequently for the manufacture of SERS-active nanoparticles.[46,47] Nanoparticles of all three metals exhibit plasmon activity in the greater part of the visible and near-IR wavelength ranges used in most Raman measurements.

Metal nanoparticles as colloids or deposited on a substrate degrade with time, because the metal surface is not protected and can be oxidized; also, nanoparticle agglomeration is possible.[48,49] Therefore, hybrid materials in which the nanoparticles are stabilized by the matrix (matrix isolated) have been developed for SERS. The possible matrices include silicon dioxide,[50] diamond-like carbon,[51] titanium dioxide,[52] graphene oxide,[53] polymers (organic and inorganic; ceramic-forming) and other dielectric or semiconductor materials.[54–58] Examples of using various matrices are shown in Fig. 8.

While developing SERS-active substrates, researchers pay much attention to monometallic nanoparticles.[60–63] However, it was found that noble metal alloys have some advantages.[64–67] Indeed, gold is superior over other metals for biomedical applications due to high biocompatibility and chemical stability, while silver provides the most pronounced SERS throughout the whole visible spectral range due to much higher (as compared with Au) plasmon resonance absorption cross-section.[68] The bimetallic Au–Ag nanoparticles are of particular interest since they are able to provide both high enhancement factors and good biocompatibility and chemical stability. Furthermore, these particles may show a tunable plasmon resonance band in the range from $\sim$410 (Ag) to $\sim$520 nm (Au) depending on the ratio of the metals, which allows the manufacture of the desired nanoparticles for different SERS excitation wavelengths.[69,70]

Development of new methods for the synthesis of hybrid SERS-active nanostructures for the most important biomedical applications (diagnosis, visualization, therapy and drug delivery) is a promising trend of modern research. The SERS labels consisting of a hybrid material with a Raman-active substance and a molecule capable of specific binding to test biological objects (antigen–antibody, ligand–receptor, enzyme–inhibitor) have a number of advantages over fluorescent labels, as they are more sensitive (in some cases, by more than three orders of magnitude) towards detection of biological molecules. Yet another substantial advantage is the multiplex ability to detect biomolecules due to narrow spectral groups in the Raman spectrum.

Carbon appears to be beneficial as the matrix, which not only prevents degradation of nanoparticles in the environment but also provides good biocompatibility due to chemical inertness.[17,71–73] The carbon–gold–silver triplex can be successfully used as SERS-labels for biological mole-

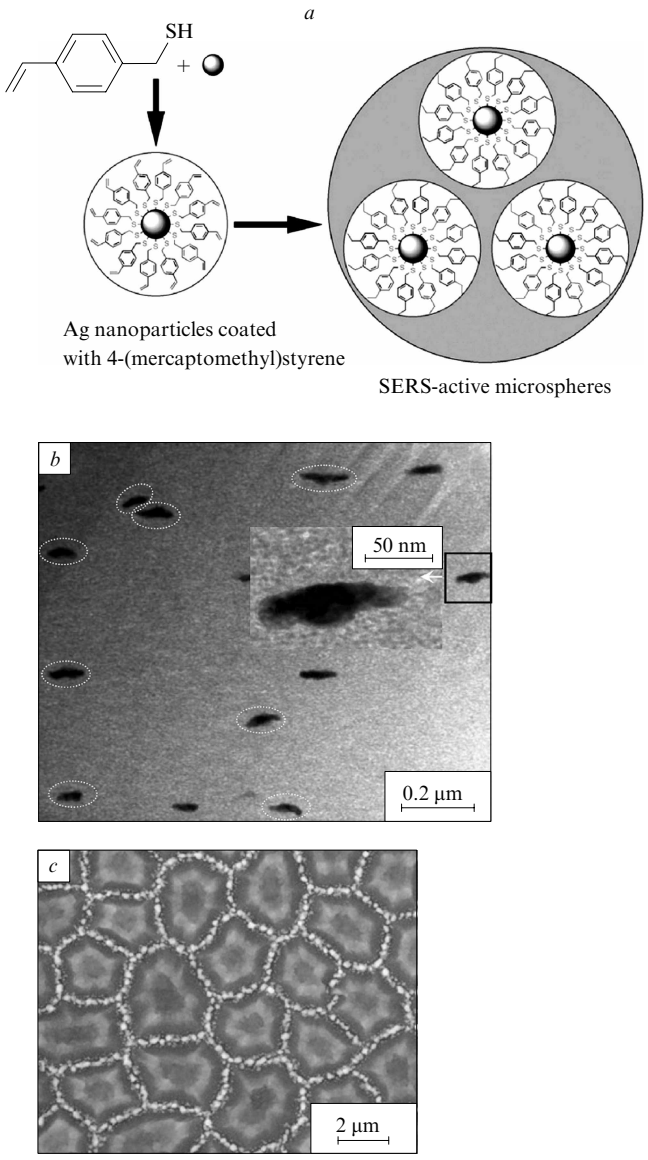


Figure 8. Examples of matrices used for noble metal nanoparticles.[59]
(*a*) Ag nanoparticles in the 4-(mercaptomethyl)styrene matrix,[38] (*b*) Au nanoparticles encapsulated in the mesoporous γ-Al_2O_3 matrix, (*c*) Ag nanoparticles in the pores of structured silicon.

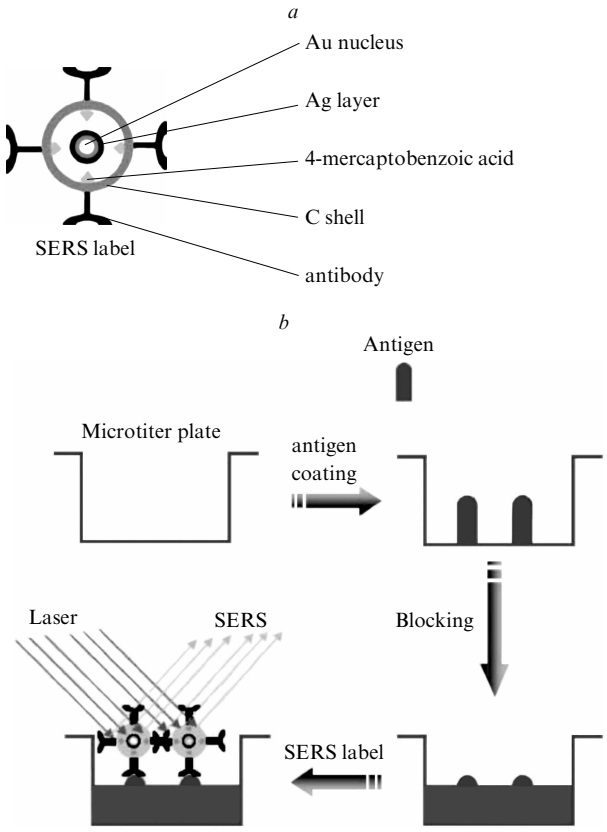


Figure 9. Schemes of the SERS label as the Au@Ag@C triplex (*a*) and SERS-based immunoassay microtitration procedure (*b*).[17]

cules. The model structure of such triplex and its application are depicted in Fig. 9.

In order to fabricate this hybrid, a gold nanoparticle of diameter 40 nm was coated with silver. The Raman-active substance, 4-mercaptobenzoic acid, was added to the core–shell structure and the whole resulting structure was coated with carbon. Such a label is attached, for example, to a mouse antigen by means of an antibody.

In order to endow nanoparticles with the desired optical properties and to increase the SERS efficiency, it is important to arrange the nanoparticles on the surface of 2D or 3D substrates (Fig. 10).

Currently, the SiO_2-Ag nanostructure is actively used as the hybrid material for SERS (Fig. 10 *a*). Silver nanoparticles are held above the surface of the underlying silver film by silicon oxide substrates. Wu and Cunningham[75] studied the relationship between the silver nanoparticles and the underlying silver film and also the dependence of the SERS enhancement factor on the thickness of SiO_2 substrates (Fig. 11).

It was found that the maximum enhancement of the SERS signal is attained when the SiO_2 substrate is 20 nm thick and the number of 'hot spots'† is maximized. This is attributable to very strong coupling between the localized surface plasmons on silver nanoparticles and the surface plasmonic polaritons on the silver film surface. This strong coupling induces a sixfold increase in the number of hot spots with respect to that in the structure with a 10 nm thick SiO_2 substrate. The greatest enhancement factor for the rhodamine 6G (R6G) spectra for the presented hybrid nanostructures is 10^9 (Fig. 11 *a*).

The attainment of the analytical limit of detection by SERS is the central issue of nanoplasmonics. Investigations of single molecules by surface-enhanced Raman spectroscopy made a revolution in the visualization and manipulation of single cells.[80–82]

By means of SERS-active porous nanostructures, it is possible to detect and identify bioorganic compounds almost at the molecular level (15–20 molecules). The hybrid structures shown in Fig. 10 *c*, which consist of porous alumina membranes with gold nanoparticles inside,

† Contact sites between single nanoparticles arise mainly in aggregates and have a stronger local electromagnetic field than single nanoparticles.[79]

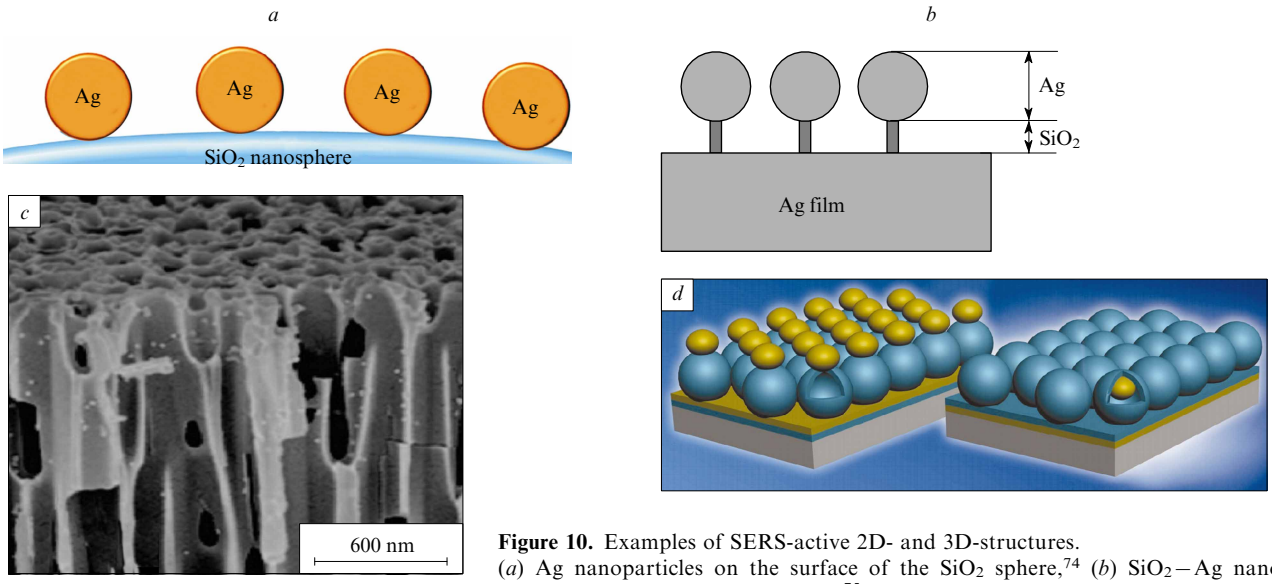


Figure 10. Examples of SERS-active 2D- and 3D-structures. (*a*) Ag nanoparticles on the surface of the SiO_2 sphere,[74] (*b*) SiO_2–Ag nanostructure on the silver film surface,[75] (*c*) vertical section of the Al_2O_3 membrane with Au clusters inside the cavities,[76] (*d*) schematic view of the Ag nanoparticles on the surface of (on the left) and inside (on the right) ZnO spheres.[77]

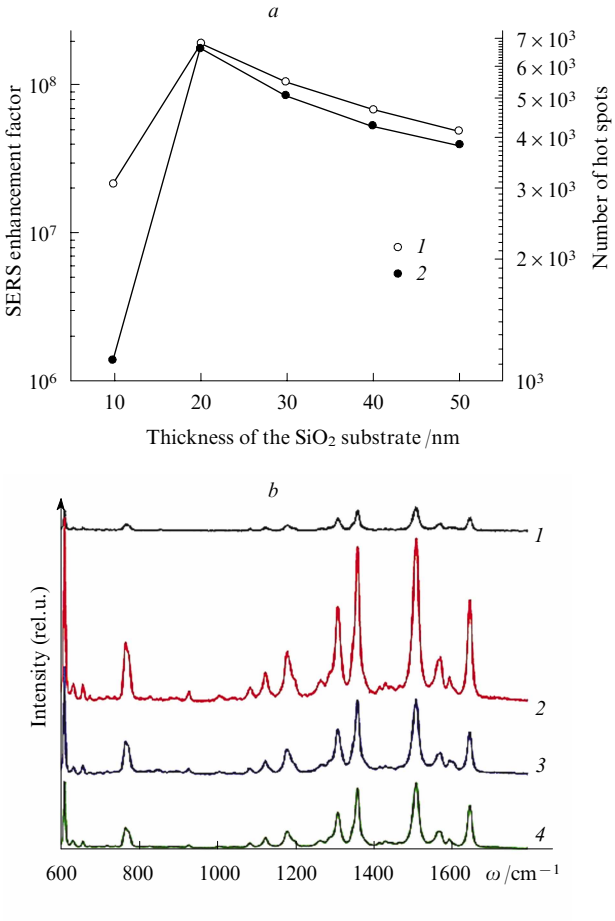


Figure 11. SERS enhancement factor (*1*) and number of hot spots calculated by the finite difference method (*2*) *vs.* the thickness of the SiO_2 substrate (*a*)[78] and SERS spectra of rhodamine 6G (1 mol litre^{-1}) on hybrid SiO_2–Ag nanostructures at the thickness of the SiO_2 substrate of 10 (*1*), 20 (*2*), 30 (*3*) and 40 nm (*4*) (*b*).[75]

were used to study explosives — 2,4-dinitrotoluene and hexamethylene triperoxide diamine (HMTD). The molecules of this compounds are non-resonance, which restricts the applicability of SERS for plastic and liquid explosives. However, the use of particularly hybrid nanostructures brought about the success in this field: the SERS signal of very low concentrations of explosives (down to ~15–20 molecules) was obtained in the area of laser beam exposure (Fig. 12).

This low limit of detection was reached owing to the use of membranes with cylindrical pores (~30 μm in diameter), which provide wave-guiding properties and, as a consequence, multiple interaction of the laser radiation with the internal surface of cylindrical pores decorated by 'hot' clusters of gold nanoparticles. Actually, this is transition from planar SERS-active substrates to three-dimensional ones.

Experimental and theoretical studies demonstrated that structures having metal nanoparticles inside the sphere or on the sphere surface (see Fig. 10 *a*,*d*) can enhance the local fields in the site of contact of the metal nanoparticle with the surface of ZnO or SiO_2 spheres due to asymmetry of the dielectric medium.[77]

III.1.b. Enhancement of luminescence

Luminescent nanoparticles are promising for the use as hidden labels for protection of documents, UV converters for light emitting diodes and solar concentrators and in medicine — for fluorescent imaging, diagnosis and therapy of diseases, selective identification of cellular and tissue structures and development of systems for remote control over molecular reactions in the cells (optogenetics), *etc.*

The surface plasmon resonance of metal nanoparticles is a unique phenomenon, which has stimulated the advent of new potent analytical methods and applications. Among these, luminescence enhancement is promising. Hybrid nanosystems contain, as a rule, actively luminescing species (lanthanide ions, quantum dots and so on), the properties of which are enhanced by plasmonic nanoparticles.[83–90] In

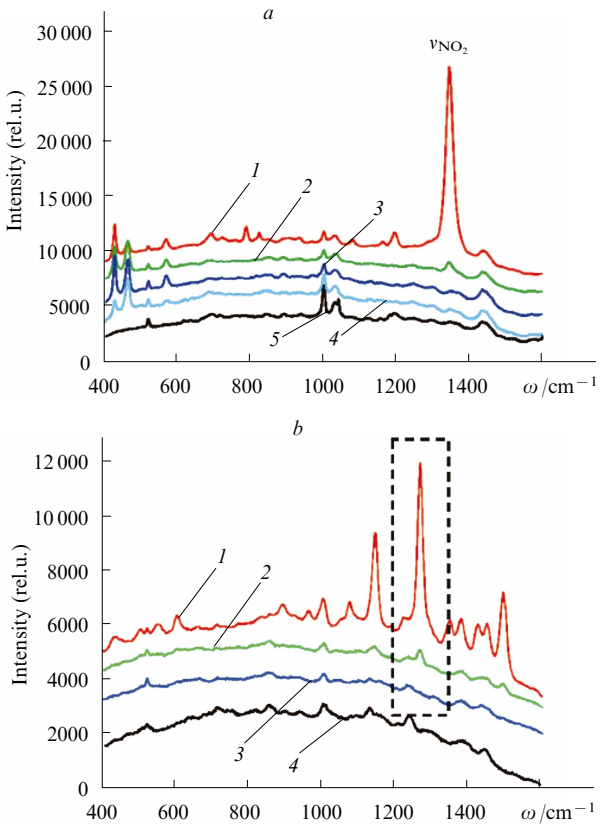


Figure 12. SERS spectra of 2,4-dinitrotoluene (*a*) and HMTD (*b*) recorded on hybrid nanostructures at different concentrations of the compounds.[76]
(*a*) Concentration of 2,4-dinitrotoluene, ppm: (*1*, *3*) 100, (*2*, *4*) 1, (*5*) substrate; (*b*) concentration of HMTD, ppm: (*1*) 100, (*2*) 10, (*3*) 1, (*4*) substrate. The dashed line marks the characteristic peaks of HMTD.

these systems, luminescence is enhanced due to the excitation of the corresponding surface metal plasmons (accompanied by electron transfer from metal nanoparticles to luminescent-active ones, *i.e.*, an increase in the dipole moment) and to an increase in the local electromagnetic field. Most frequently used forms of luminescent hybrids are nanorods/nanofibres decorated with metallic and luminescent nanoparticles (Fig. 13 *a*,*b*) and core–shell nanoparticles (Fig. 13 *c*–*e*) in which either a metal nanoparticle or the active luminescent compound can serve as the core.

The up-conversion luminescence, which allows conversion of IR radiation into visible light, by means of two- or multi-photon absorption, attracts researchers' attention as it could serve for the design of up-conversion lasers, quantum IR counters, 3D displays and for *in vivo* fluorescence visualization.[93–97]

Among up-conversion luminophores, some lanthanide ions used in pairs (for example, Er^{3+}/Yb^{3+} or Tm^{3+}/Yb^{3+}) are most efficient upon excitation at $\lambda = 980$ nm due to the sufficient absorption at appropriate energy levels and low phonon energy, which induces relatively intense up-conversion luminescence.[98] Nevertheless, the tasks of increasing the conversion efficiency upon frequency increase, enhancement of absorption band intensity and control of the concentration and temperature quenching of luminescence are topical. For this purpose, hybrid nanostructures $Ag–SiO_2–Er_2O_3$ (Figs 13 *c* and 14) were developed.[71]

Silver nanoparticles have an average size of about 60 nm (Fig. 14 *a*); after deposition of a SiO_2 layer, the particles become monodisperse and have a core–shell structure. The SiO_2 shell is 10–15 nm thick. After deposition of the Er_2O_3 coating, the size of spherical $Ag–SiO_2–Er_2O_3$ nanostructures varies from 150 to 200 nm (see Fig. 14 *c*).

As a result of interaction between Er_2O_3 and surface plasmons of the Ag nanoparticle, the following parameters were increased: the spectral width of the excitation band and the intensity of up-conversion luminescence (up to 10^4-fold), which depends appreciably on the power density of the excitation light (Fig. 15).

Figure 15 *a*,*b* shows the up-conversion luminescence spectra of Er_2O_3 nanoparticles and $Ag–SiO_2–Er_2O_3$ nanostructures under the excitation intensity from 0.26 to 1.41 W mm^{-2} ($\lambda = 980$ nm). It can be seen that at relatively low laser intensity, the emission spectra have narrow-band transitions at 550 and 660 nm. As this parameter increases, a broad luminescence band is observed with a maximum at 600 nm. The mechanism of its appearance has not been

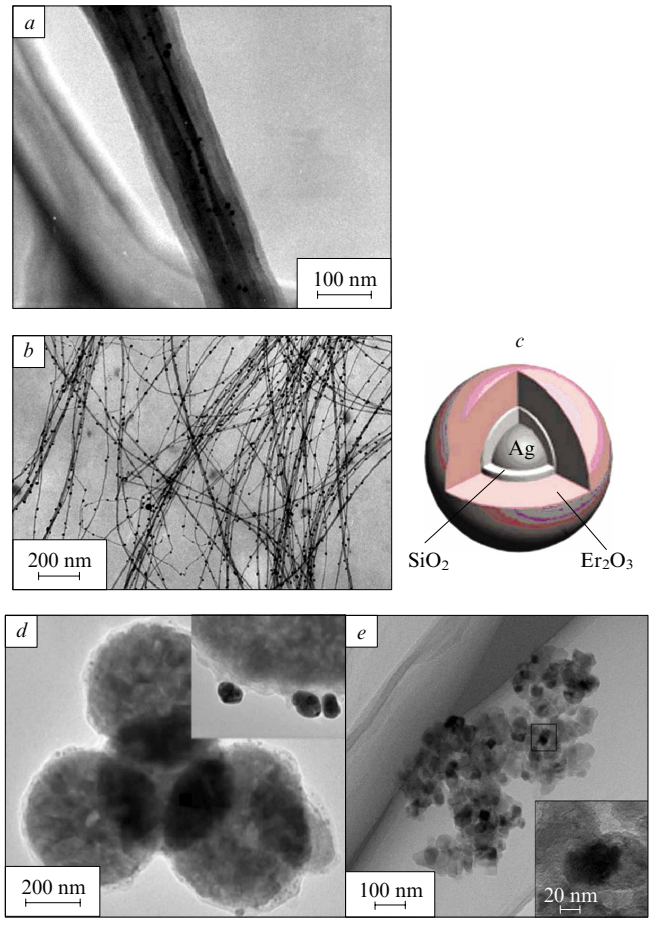


Figure 13. Examples of hybrid luminescent nanostructures.
(*a*) SiO_2 : Eu(TTA)$_3$phen nanofibres (TTA = $C_8H_5F_3O_2S$, phen = $C_{12}H_8N_2$),[84] (*b*) CdSe nanofibre decorated with Au nanoparticles,[87] (*c*) $Ag–SiO_2–Er_2O_3$,[91] (*d*) Y_2O_3 : Er@Au,[92] (*e*) gold nanoparticles coated with TiO_2.[85]

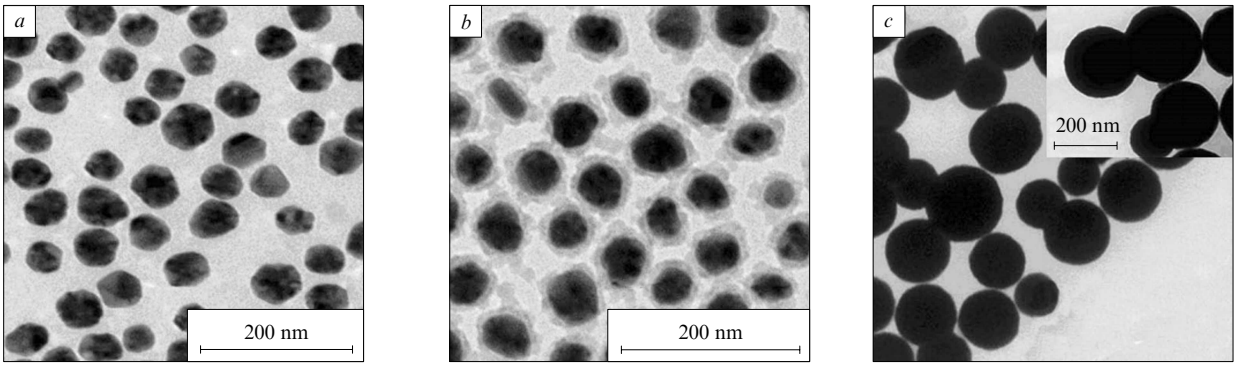


Figure 14. TEM images of silver nanoparticles (*a*), $Ag-SiO_2$ structures (*b*) and $Ag-SiO_2-Er_2O_3$ structures (*c*).[91]

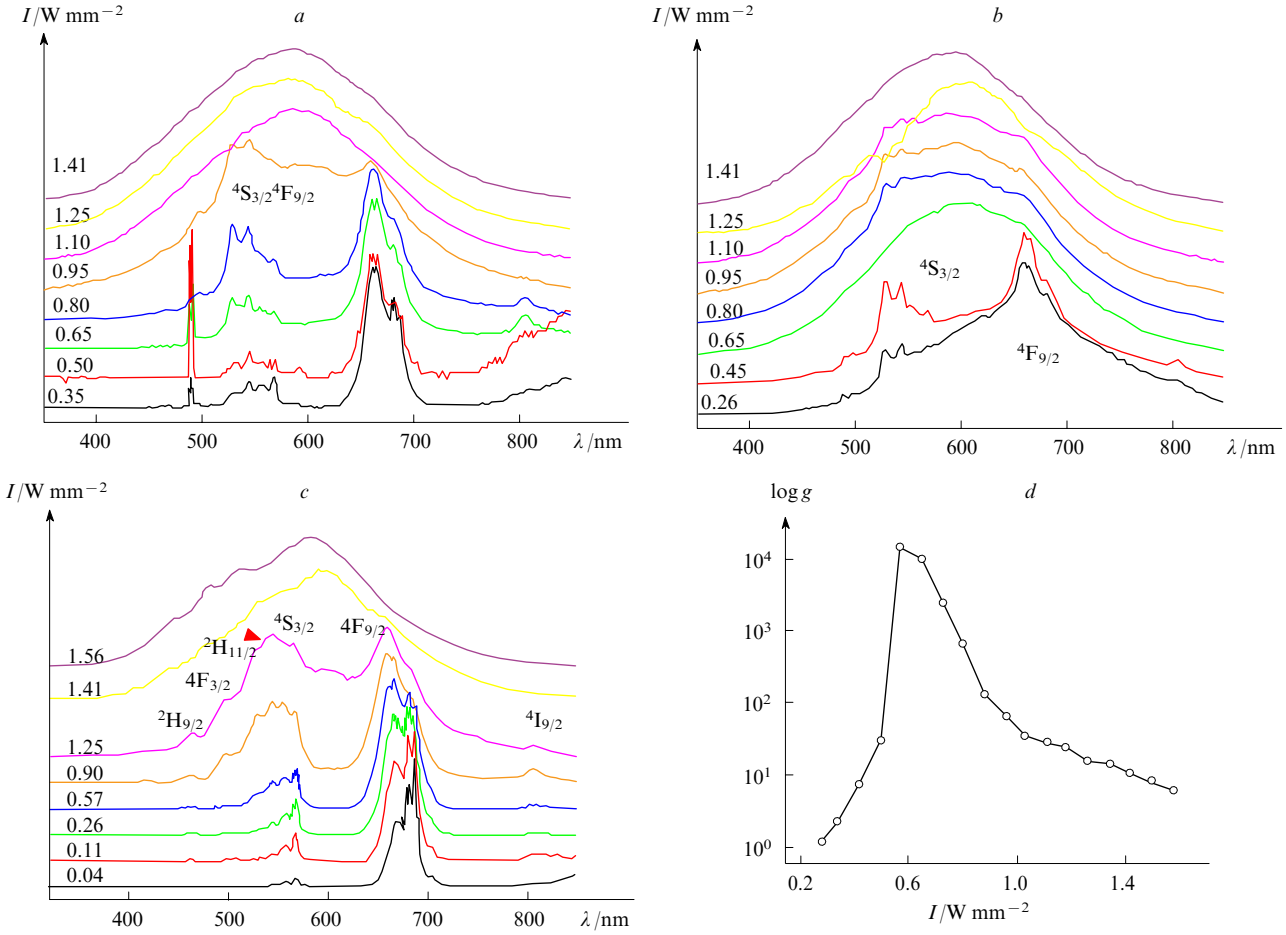


Figure 15. Up-conversion luminescence spectra of Er_2O_3 nanoparticles (*a*), $Ag-SiO_2-Er_2O_3$ (*b*) and bulk Er_2O_3 (*c*) depending on the excitation power density (I) at 980 nm and the enhancement factor (g) of the up-conversion luminescence *vs.* excitation power (*d*).[91] Indicated in the curves are the excitation radiation intensities (values) and the energy levels from which luminescence takes place.

established as yet and is a matter of discussion. Luminescence enhancement is related to the following factors:[71]

— at $\lambda = 780-980$ nm, the corresponding silver surface plasmons are excited, which is accompanied by electron transfer from Ag nanoparticles to Er_2O_3 and the dipole moment of Er_2O_3 increases, thus enhancing the up-conversion luminescence;

— due to the increase in the local electromagnetic field, pumping and emission increase;

— the thermal effect is summed up with the excitation of the surface plasmons of Ag nanoparticles and this results in a decrease in the excitation threshold of broad-band emission.

Research of small-size semiconductors is related to their potential application in nanoelectronics. Among these material, zinc oxide attracts attention by its multifunctional properties, which have found use in solar cells, UV lasers and light detectors, photocatalysts and gas sensors.[99–106]

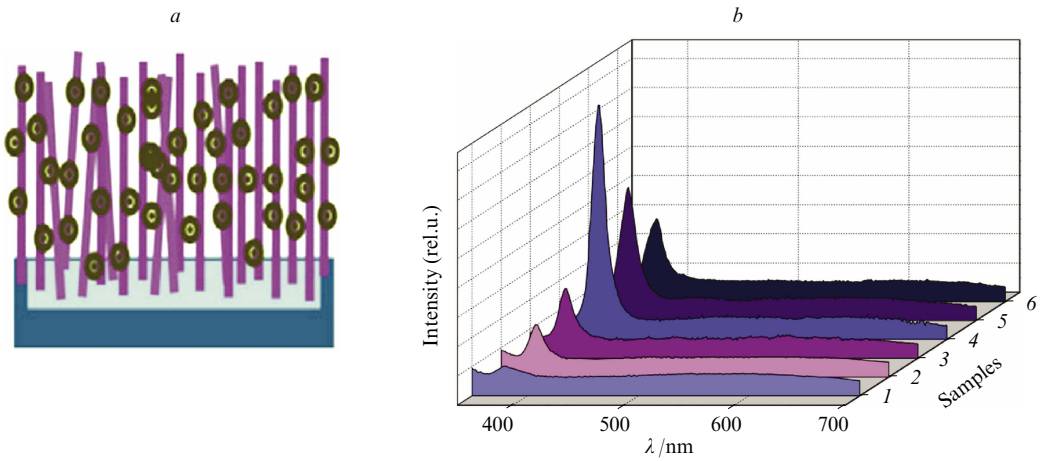


Figure 16. Schematic view of ZnO nanorods decorated with Cu nanoparticles (*a*) and luminescence spectra at room temperature (*b*).[83] Sample: (*1*) ZnO nanorods, (*2–6*) ZnO nanorods with different contents of copper nanoparticles on the surface.

Owing to high exciton binding energy (60 meV), intense UV radiation can be obtained from ZnO upon radiative recombination of excitons at room temperature and at higher (up to 550 K) temperatures.[107] Currently, active research is carried out into enhancement of spontaneous radiation of ZnO by aluminium,[108, 109] platinum,[108, 110, 111] gold [112–116] and titanium [117, 118] nanoparticles. The enhancement factor of spontaneous radiation varies over a broad range and depends on various parameters, in particular, on the metal nanoparticle concentration, shape and composition. Liu *et al.*[119] reported the procedure for optimization of the concentration of Ag nanoparticles in poly(methyl methacrylate) (PMMA) to obtain efficient UV electroluminescence of light-emitting diodes based on p-GaN/n-ZnO heterostructures. It was found that under the action of Ag nanoparticles, the contribution of ZnO excitons to the electroluminescence of light emitting diodes increases more than 13-fold and the spectral line shape changes. Furthermore, using silver nanoparticles for light emitting diodes, it was possible to improve the spatial uniformity and to increase the output photon intensity and the angular distribution of the emission almost twofold.

Interesting studies were concerned with the decoration of ZnO nanorods with copper nanoparticles and the dependence of the luminescence of this hybrid on the content of copper nanoparticles on the surface (Fig. 16 *a*). Hybrid nanostructures were prepared in the following way: 50, 100, 150, 200 and 250 μl (for samples *2–6*, respectively) of a colloid solution of copper nanoparticles in methanol was added to 5 ml of polyethylene glycol (PEG), and ZnO nanorods were decorated from the resulting solutions by centrifugation.

The photoluminescence characteristics of ZnO nanorods without decoration (*1*) and with decoration (*2–6*) by copper nanoparticles are shown in Fig. 16 *b*. The luminescence spectra of ZnO nanorods exhibit an intense UV peak at 380 nm (3.26 eV) associated with recombination of excitons and a broad band in the visible region (400 to 700 nm) associated with electron–hole recombination in surface or bulk defective layers. The decoration of nanorods with copper nanoparticles changes the position of the UV peak in the absorption spectrum from 379 to 386 nm. The peak displacement to longer wavelengths can be due to coupling between ZnO excitons and localized surface plasmons.[120] After introduction of copper nanoparticles, the intensity of the UV peak increases with increase in the nanoparticle concentration up to sample *4*, other conditions of luminescence excitation being the same. The luminescence intensity of sample *4* is eight times higher than that of ZnO nanorods not decorated with copper nanoparticles. On further increase in the concentration of copper nanoparticles, the luminescence intensity decreases but still remains higher than the luminescence of ZnO nanorods. Annealing at 500 °C additionally enhances (up to 9-fold) the luminescence intensity with respect to that of the initial nanorods. The luminescence enhancement after decoration of nanorods was attributed to coupling of the spontaneous ZnO radiation with the arising surface plasmon resonance of copper nanoparticles. If the semiconductor band gap is comparable with the plasmon energy at the metal/semiconductor interface, the electron–hole pair recombination may give rise to photon emission that would be in resonance with the plasmon vibration modes.[83]

III.2. Catalytically active hybrid nanostructures

Quite a few multifunctional hybrid nanostructures that, along with the SERS activity, demonstrate also photocatalytic properties have been developed to date. As a rule, these are combinations of noble metals and semiconductor materials such as Ag and Au/TiO_2 (Refs 121 and 122) or Au/ZnO (Ref. 123). In the studies of these structures, the attention is focused on their photocatalytic activity towards the photodegradation of organic pollutants or cleavage of water molecule.[124–127] Zinc oxide is a direct wide-band semiconductor with a high excitation energy, which (like TiO_2) shows high performance in a photocatalytic reaction. Apart from well-known applications, ZnO has found use in sensitized dyes for solar batteries.[127–129] The photocatalytic effect of the metal/semiconductor hybrid nanostructures can be markedly enhanced in the following way:[130–133]

— increase in the light absorption of the semiconductor due to overlap of the plasmon resonance energy of the metal nanoparticle and the fundamental absorption edge of the semiconductor;

— decrease in the diffusion length of the electron–hole pair in the nanostructure;

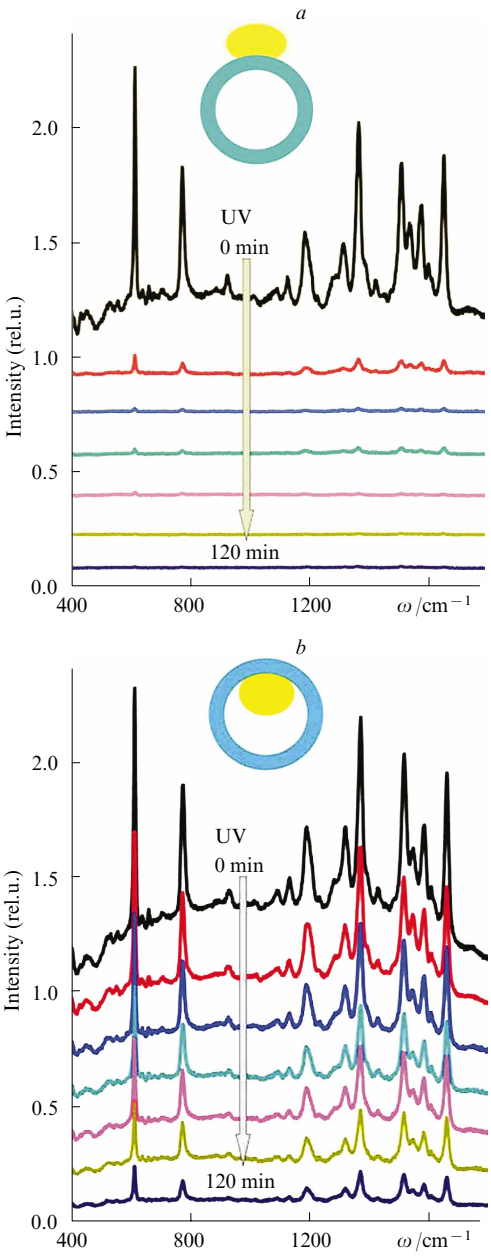


Figure 17. SERS spectra of the R6G sample (10^4 mol litre^{-1}) on nanostructures of various structure upon UV irradiation for 120 min.[77]
(*a*) Ag is on the ZnO surface, (*b*) Ag is inside the ZnO sphere.

— forced separation of the electron–hole pairs upon the transfer of high-energy electrons between the metal and the semiconductor.

The photocatalytic activity of Ag/ZnO nanostructures (see Fig. 10 *c*) on exposure to visible and UV light was estimated from the intensity of Raman scattering of an R6G sample.[73] In the photocatalytic process, a Philips lamp (18 W) emitting lines from 340 to 410 nm with a maximum at 365 nm served as the UV source. As the source of visible light, a xenon lamp (500 W) with an UV filter was used. The Raman spectrum was recorded at 488 nm. The UV radiation-induced photodegradation of R6G can be monitored by the SERS spectra of a R6G sample presented in Fig. 17.

It can be seen that for both structures, the Raman signal intensities of the R6G sample decrease with increase in the irradiation time, the most rapid photodegradation of R6G being observed for the Ag/ ZnO structure. On exposure of the system to visible light, the situation changes, and the Ag@ZnO structure becomes most efficient. Hong and Li,[62] who studied the mechanism of R6G degradation, proposed a model of electron transfer based on equalization of the band gap width.

Nanostructured materials have a highly developed surface; therefore, they are promising for the elaboration of heterogeneous catalysts. Of particular interest are catalysts containing metal nanoparticles (Pt, Pd, Au, *etc.*) or metal compounds (a widely known example is Al_2O_3). Placing the nanoparticle catalysts into a matrix (carbon, mesoporous silicon, polymer) prevents them from aggregation, increases the performance and selectivity of the catalytic reaction.

Considering the application as catalytically active materials, highly attractive are hybrid nanostructures consisting of a porous carbon matrix with encapsulated metal nanoparticles. Tang *et al.*[134] investigated the catalytic properties of Au–Pd nanoparticles encapsulated in carbon nanospheres (Fig. 18). The catalytic properties of the presented hybrid structures were tested in the reduction of 4-nitrophenol with $NaBH_4$. The progress of the reaction was followed by absorption spectroscopy (Fig. 19). In the absence of a catalyst, the 4-nitrophenol concentration does not decrease (the maximum absorption peak at 400 nm does not change and the mixture remains yellow-coloured). Upon the addition of Au–Pd/C hybrid nanostructures, the concentration of 4-nitrophenol decreases and the solution is bleached. The catalytic activity depending on the gold to palladium ratio in the test series of samples was maximum at Au : Pd = 2.1. It was shown that the catalysts can be used once again and the reaction rates remain almost unchanged in the subsequent cycles.

The increase in the catalytic properties of hybrid nanostructures was demonstrated [135] in relation to electroreduction of oxygen. The polarization curves of oxygen reduction catalyzed by various structures are shown in Fig. 20. The curves were constructed by normalization of the electric current that passes through the graphene/glassy carbon electrode to the mass of platinum deposited on the glassy carbon surface. It can be seen that the oxygen reduction occurs at a much higher rate in the presence of hybrid catalysts. The authors attributed the increase in the catalytic activity of Pt–Au–graphene structures with respect to the activity of the Au–graphene or Pt–graphene structures to the fact that platinum nanoparticles grow on gold nanoparticles, which substantially increases the active surface area.

Due to the specific structure and morphology, hybrid nanostructures can function as space-confined chemical reactors. For example, core–shell nanostructures with vacant space between the core and the shell were considered [136] as nanoreactors for selective oxidation of alcohols. The key idea is the use of molecular oxygen as the oxidant instead of metal oxides used in industry, which are usually toxic and expensive. Mesoporous organosilicon shells with Pd nanoparticles were proposed as hybrid structures (Fig. 21). The results of oxidation of various alcohols by this method are summarized in Table 2. The oxidation was carried out at 50 °C for 8 h. As can be seen in Table 2, all

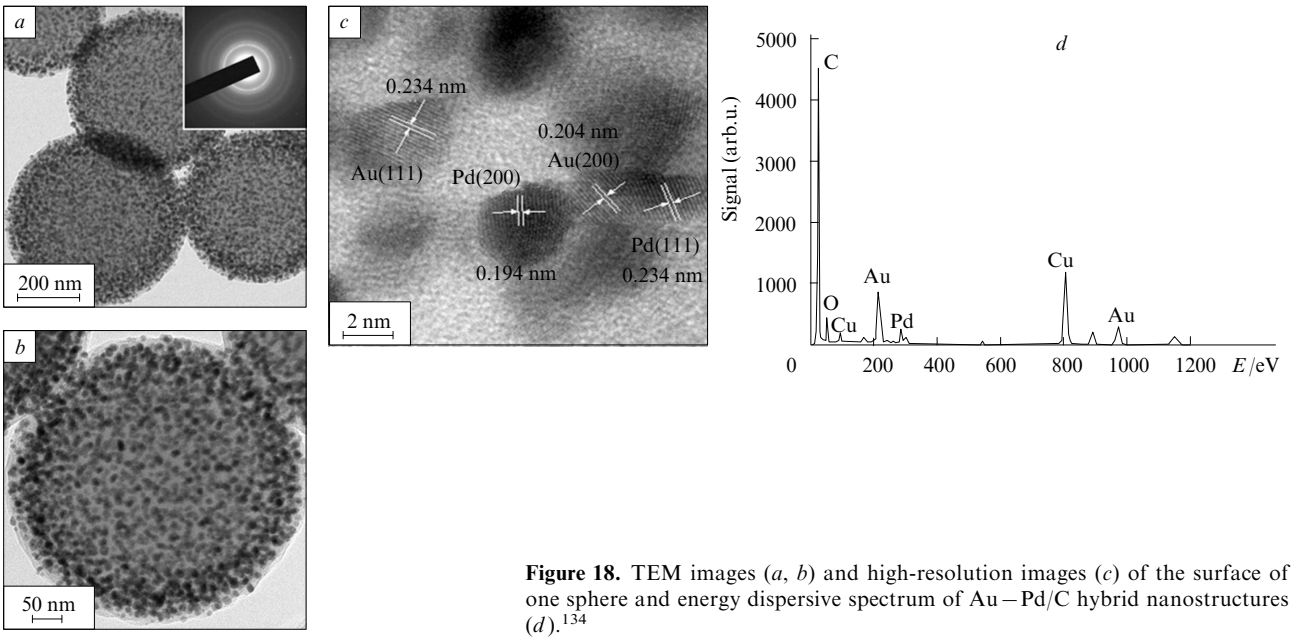


Figure 18. TEM images (*a*, *b*) and high-resolution images (*c*) of the surface of one sphere and energy dispersive spectrum of Au–Pd/C hybrid nanostructures (*d*).[134]

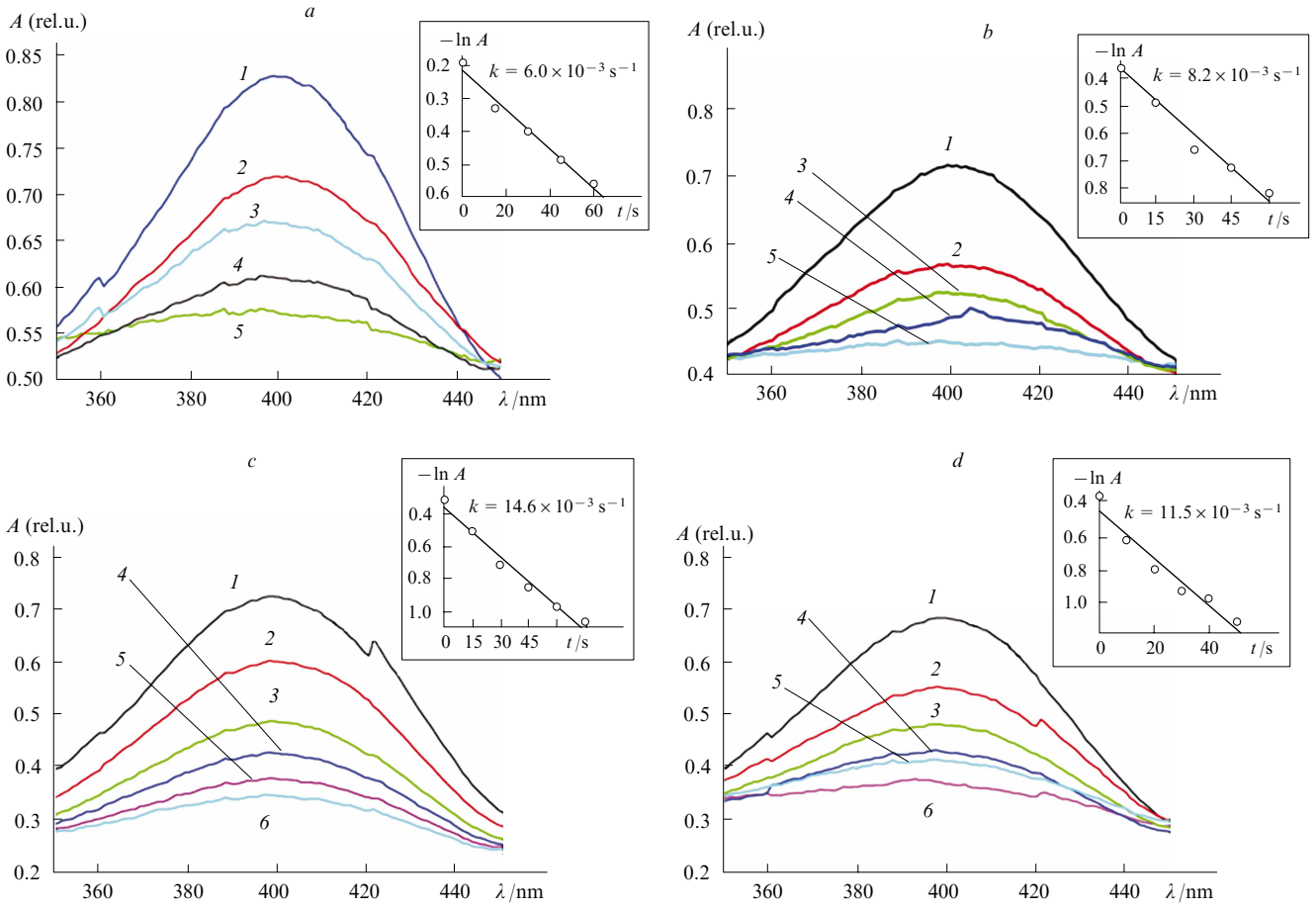


Figure 19. Absorption spectra demonstrating the decrease in the 4-nitrophenol concentration (reduction with $NaBH_4$) in the presence of Au–Pd/C hybrid nanostructures with the Au : Pd ratio of 0.4 (*a*), 1.2 (*b*), 2.1 (*c*) and 3.4 (*d*). The insets show the dependences of the logarithm of the extinction coefficient at 400 nm on the reduction time; *k* is the reaction rate constant.[134]
t/s: (*a*, *b*) 0 (*1*), 15 (*2*), 30 (*3*), 45 (*4*), 60 (*5*); (*c*, *d*) 0 (*1*), 10 (*2*), 20 (*3*), 30 (*4*), 40 (*5*), 50 (*6*).

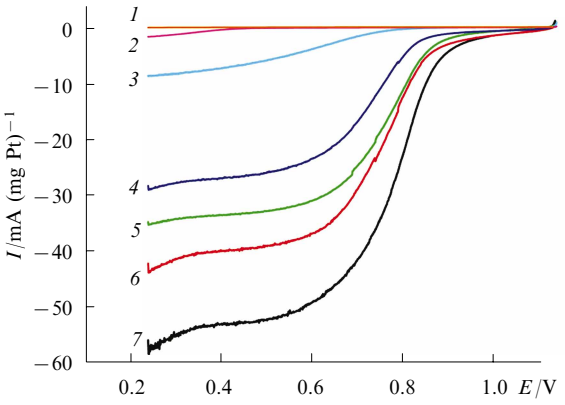


Figure 20. Polarization curves for oxygen reduction with graphene (*1*) and hybrid nanostructures: Au–graphene (*2*), Pt–graphene (*3*), Pt–Au–graphene with the Pt : Au molar ratio of 0.5 : 1 (*4*), 3 : 1 (*5*), 1 : 1 (*6*) and 2 : 1 (*7*) in 0.5 M H_2SO_4 saturated with oxygen with stirring at 1600 rpm; sweep rate 10 mV s^{-1} (see Ref. 135).

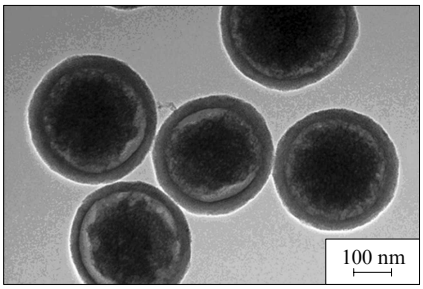
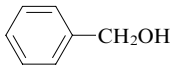
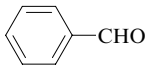
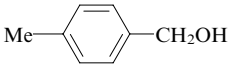
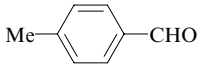
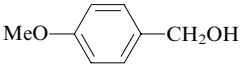
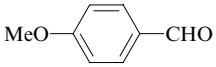
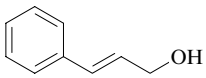
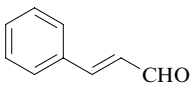
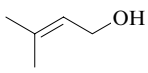
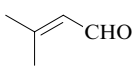


Figure 21. TEM image of Pd nanoparticles with mesoporous organosilicon shells.[136]

Table 2. Selective (>99%) oxidation of various alcohols in nanoreactors.[136]

Alcohol	Product	Yield (%)
		94
		92
		100
		100
		53

reactions are highly selective and the yields can be as high as 100% for some alcohols.

III.3. Hybrid magnetic nanostructures

The great interest of researchers in the nanoparticles having magnetic properties is related to particular applications, *e.g.*, for data recording and storage systems, for magnetic cooling, as magnetic sensors[137,138] and in medicine.[139] Indeed, in the MRI diagnosis the contrast agents are often used for the more precise determination of the boundaries, structures and types of tumours. As a rule, Fe_3O_4, dual-layer Fe@Fe_3O_4 nanoparticles of gadolinium chelate complexes, *etc.*, are typically used as such substances. In addition, under the action of external magnetic field, magnetic nanoparticles can be targeted to definite organs to reach a specified concentration in them and a specified time of action and, after that, to be excreted from the body. This approach not only increases the quality of MRI examination but also realizes the targeted drug delivery concept and reduces the general toxic effect of drugs; moreover, it can induce controlled heat effects in specified sites (hyperthermia). In the last-mentioned case, the introduction of magnetic nanoparticles into a particular area of the body (*e.g.*, into a malignant tumour) and application of a magnetic field can induce local heating and the subsequent destruction of the tumour cells. The magnetic nanoparticles used in medicine most extensively are compounds based on iron, cobalt and nickel and their oxides such as magnetite Fe_3O_4, maghemite γ-Fe_2O_3, cobalt ferrite $CoFe_2O_4$, chromium dioxide CrO_2, *etc.*

Analysis of the latest studies dealing with magnetic nanoparticles demonstrated that ever increasing interest is shown in complex modified systems: magnetic nanoparticles incorporated into some matrix. In this system, nanoparticles are stabilized, the variability of their applications and the biochemical compatibility (for retardation and control of the excretion from the body — phagocytosis) can be increased and the functional properties of the system can be extended by endowing the matrix with specific properties. Stabilization of magnetic nanoparticles upon encapsulation into bulk materials (glasses, polymers, xerogels and silica gels, zeolites and so on) is the subject of several publications (see, for example, Ref. 137). This review places emphasis on hybrid magnetic nanostructures (HMN), which remain in the nano-sized range and, hence, are suitable for specific applications, first of all, for solving biomedical problems.

III.3.a. Targeted drug delivery

A very important application of HMN is the targeted drug delivery, most often, when the therapy of the disease requires treatment of tumours of various aetiology. Modern antitumour agents are quite efficient; however, they affect not only tumour but also healthy cells; therefore, some of the developed antitumour agents have not found clinical use. The toxic action on the body can be reduced by precise delivery of drugs into the damaged site by means of so-called nanocarriers — nanoparticles carrying drugs. The targeted drug delivery may be either active or passive:[122]

— the passive delivery is based on enhanced penetrability of the damaged sites in the body and the accumulation effect related to it;[140,141]

— active delivery implies coating of nanocarriers with specific molecules (proteins, peptides or antibodies) having high affinity for tumour cells and thus providing efficient targeting of the drugs.

Drug-containing nanoparticles may incorporate magnetic nanostructures, which offer additional opportunity for manipulating them by means of external magnetic fields.

Hybrid magnetic core–shell nanostructures. One type of HMN used for targeted drug delivery are core–shell structures. In these systems, the core is formed by nanoparticles possessing magnetic properties (Fe, Co, Ni, iron oxide), while the shells, which have good biocompatibility and provide the possibility to attach drugs, can consist of various elements or compounds (Au, SiO_2, polymers, organic compounds).[142–144] A different morphology is possible: for example, gold nanoparticles with molecular magnets being deposited on the surface.[145]

The scheme of a complex multilayer core–shell HMN is shown in Fig. 22. The multilayer shell makes it possible to load the drugs and to isolate them from other system components and makes the structure biocompatible. Folic acid ensures the active targeted delivery, while doxorubicin (anthracycline antitumour antibiotic) serves as the drug.

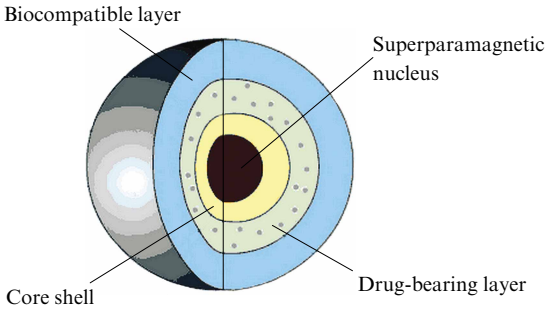


Figure 22. Example of a magnetic multilayer core–shell structure for targeted drug delivery.[146]

When the core contains a superparamagnetic Fe_3O_4 nanoparticle, it is possible not only to control HMN but also to release the drugs *via* controlled heating of HMN under the action of an external alternating magnetic field. It is noteworthy that the procedure of synthesis of these structures is fairly complicated and multistage: apart from the formation of a core with a specified composition, structure and morphology, it is necessary to load the controlled amount of the chosen drug, to form the biocompatible coating and to functionalize the surface by specific molecules.

Hybrid magnetic nanostructures based on carbon nanostructures. One more approach that provides both the targeted drug delivery and more effective synthetic procedure is the development of HMN based on magnetic nanoparticles encapsulated in various carbon nanostructures. Carbon allotropes possess a variety of interesting properties, that is why carbon is called 'material of the 21st century'. Carbon nanostructures can be obtained as single- and multi-walled nanotubes, fullerenes, graphene and so on.

A carbon allotrope — graphite — is a three-dimensional structure consisting of numerous graphene layers. Oxidation of graphite with strong oxidants gives rise to graphite oxide with increased distances between the carbon layers; finally, this material acquires hydrophilic properties. For example, sonication of graphite oxide in water may afford graphene oxide — a structure comprising one or several layers. Graphite oxide differs from graphene oxide by the multilayer structure. A remarkable feature of graphene oxide is high specific surface area, which allows it to encapsulate various substances such as metals, biomolecules, luminescent molecules, drugs and so on.

Yang *et al.*[147] discussed the synthesis and considered the application for targeted drug delivery of a superparamagnetic hybrid material consisting of graphene oxide and magnetite nanoparticles. The magnetite nanoparticles were formed on graphene oxide plates upon chemical precipitation. The diameter of the synthesized Fe_3O_4 nanoparticles was 2–4 nm with a narrow size distribution. The resulting hybrids were found to exhibit superparamagnetic properties and can be used for drug delivery (doxorubicin was considered as an example, the loading capacity being as high as 1.08 mg mg^{-1}). Fairly important features of the graphene oxide–Fe_3O_4 nanoparticle–doxorubicin system are hydrophilic properties and the presence of functional carboxyl groups, which can serve for further attachment of active molecules to provide targeted drug delivery. In addition, the possibility of manipulating the obtained HMN by means of pH change (aggregation in an acid medium) and controlled motion under the action of an external magnetic field were demonstrated. In an alkaline medium, deaggregation takes place to form a stable suspension, which may be used for effective excretion of HMN from the body.

Carbon nanotubes are widely used carbon materials. On the one hand, application of carbon nanotubes in biology and medicine is restricted by their poor solubility in aqueous media; on the other hand, carbon nanotubes show good cell permeability and can efficiently penetrate into various organs and tissues. In addition, they are stable in various bioorganic media and, like most carbon nanostructures, they have a large surface area, which can be coated with various compounds.

A structural feature of carbon nanotubes is the presence of a cavity, which can be filled with functional components (drugs, dyes, luminescent compounds, *etc.*). Carbon nanotubes can be endowed with magnetic properties upon functionalization with magnetic nanoparticles. Carbon nanotubes with magnetic nanoparticles are exceptionally interesting objects for the task of targeted drug delivery.

Three approaches have been proposed for the design of HMN based on carbon nanotubes: deposition of magnetic nanoparticles on the surface of nanotubes (Fig. 23 *a*) [148] and insertion of magnetic nanoparticles into the cavity (Fig. 23 *b*)[149, 150] and into the nanotube walls (Fig. 23 *c*).[151] The structures obtained in this way can be subjected to subsequent functionalization by insertion of medicinal agents, deposition of active molecules and protective coats.

As regards the use of HMN for the targeted drug delivery, carbon nanotubes with magnetic nanoparticles encapsulated in their walls appear to be most interesting. These hybrid nanostructures are characterized by exceptionally high drug loading capacity, because this may involve both the outer surface and the inner cavity of nanotubes, and the possibility of additional functionalization is also retained. The synthesis of carbon nanotubes containing magnetic nanoparticles in the inner cavity is complicated, and their application is restricted by relatively low drug loading capacities. The deposition of magnetic nanoparticles on the nanotube surface provides for drug loading and additional functionalization but to lesser extent as compared with carbon nanotubes with encapsulated magnetic nanoparticles.

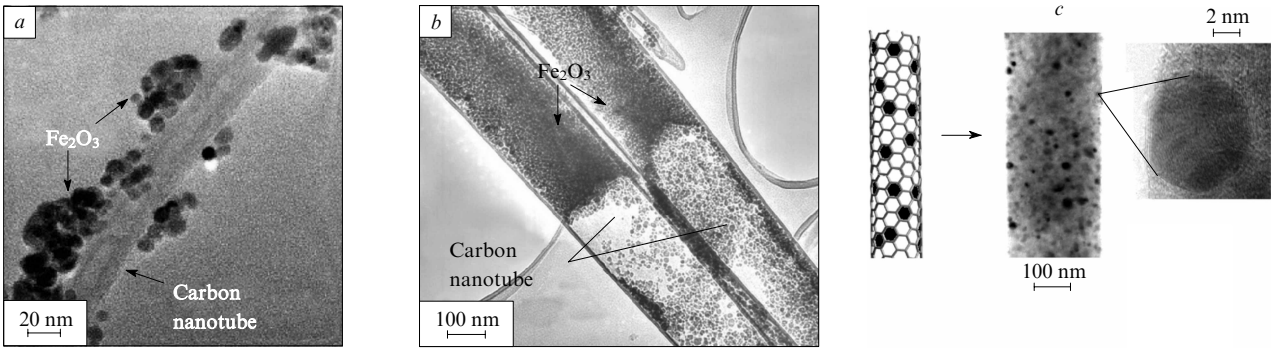


Figure 23. Hybrid magnetic nanostructures based on carbon nanotubes with magnetic nanoparticles deposited on the surface (*a*),[148] introduced into the cavity (*b*)[149, 150] and into nanotube walls (*c*).[151]

III.3.b. Cell and tissue visualization

Combination of magnetic and luminescent nanoparticles in one structure may solve simultaneously the monitoring and manipulation problems, visualize the site of pathology or follow the motion trajectories of some cells and perform the targeted drug delivery (under the influence of a magnetic field) or some local impact (*e.g.*, heating). Possible luminescent agents include quantum dots (ZnS, PbS, CdS, CdSe), organic compounds (fluorescein, Cy3, porphyrin, oligothiophene), nanocrystals with lanthanide ions and nanoparticles (Au, Ag) exhibiting plasmonic properties. Magnetic and luminescent nanoparticles can be aggregated into a single structure; a matrix can also be used for this purpose (encapsulation, insertion).

An example of the matrix-free approach to the development of HMN for tumour cell visualization has been reported:[152, 153] the CdSe and ZnS quantum dots were applied onto magnetite nanorings or nanospheres.

A specific feature of matrix-free systems is their small size as compared with sizes of the structures synthesized using the matrix approach. This is responsible for their high mobility and the possibility to achieve high resolution of tumour visualization. However, these structures tend to exhibit luminescence quenching and pronounced light absorption by magnetic nanoparticles owing to the proximate positions of the magnetic and luminescent objects. Furthermore, these structures can be fairly toxic.

The matrix approach to the design of HMN for cell and tissue visualization is more popular, because in this case, it is possible to control the morphology and the distance between luminescent and magnetic nanoparticles and, hence, to minimize the luminescence quenching effects. Polymers, SiO_2, micelles and other substances can serve as matrices.[154–157] By using a matrix, it is possible to provide more efficient functionalization of HMN systems by attaching additional components, for example, to increase the biocompatibility. Runowski *et al.*[158] considered magnetic nanoparticles and CdSe–ZnS quantum dots encapsulated into polymer micelles. The HMN thus obtained preserve both the luminescence and magnetic properties, which are determined by the constituent nanoparticles; in addition, the toxic action of CdSe is minimized.

The matrix approach has been used to prepare an HMN system based on heterodimers of silver and magnetite Janus nanoparticles coated with a SiO_2 layer.[9] In this case, plasmonic Ag nanoparticles were used as visualization centres; they are less toxic than quantum dots and, unlike organic luminophores, they show luminescence that is stable with time. An image of the Janus type structure 'magnetite nanoparticle–Ag nanoparticle–SiO_2 shell' is shown in Fig. 25. In this case, the SiO_2 matrix minimizes the toxic effect of silver nanoparticles, while in the presence of plasmonic nanoparticles, it becomes possible to extend the visualization methods by means of dark field microscopy, multiphoton luminescence microscopy, light scattering.

One more advantage of the structures based on magnetic and plasmonic nanoparticles is the possibility to carry out selective photothermal destruction of tissues by means of optical heating of metal nanoparticles upon IR excitation.[155]

The desired cells and tissues can be visualized using lanthanide ions. An important advantage of materials doped with these elements over materials containing organic dyes or quantum dots is that IR excitation can be

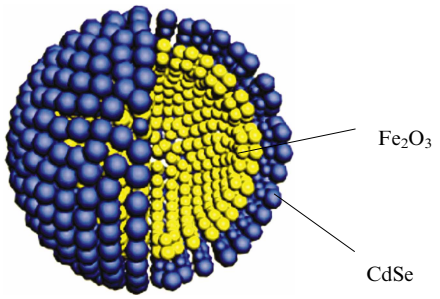


Figure 24. Scheme of HMN based on magnetite nanospheres.[143]

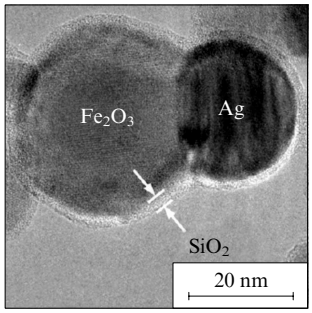


Figure 25. Janus type Fe_2O_3–Ag nanoparticle–SiO_2 shell.[9]

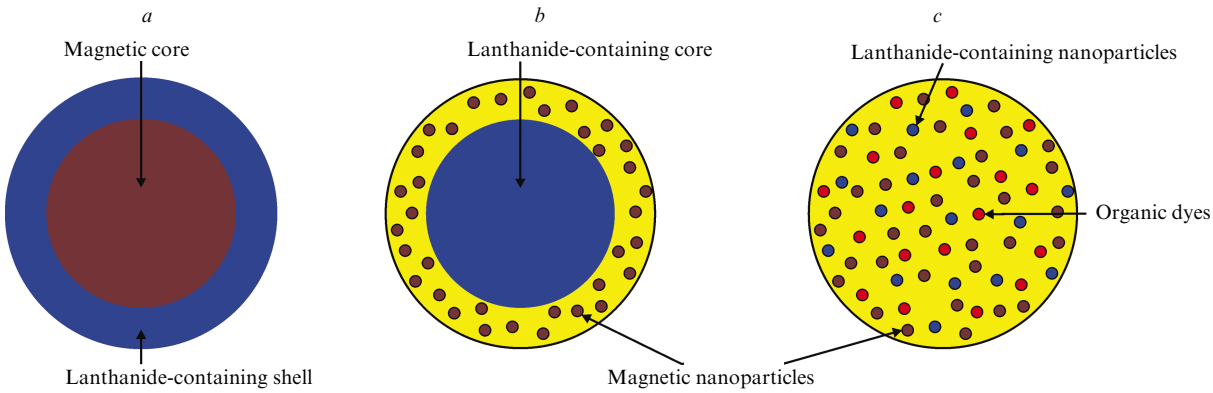


Figure 26. Examples of morphology of structures combining magnetic and luminescent nanoparticles based on lanthanides. (*a*) Core (magnetic nanoparticle)–shell (lanthanide nanoparticles) structure, (*b*) core (lanthanide nanoparticles)–shell (magnetic nanoparticles) structure, (*c*) multicomponent structures comprising magnetic nanoparticles and various types of luminescent components (organic dyes and lanthanide-containing nanoparticles).

used and the anti-Stokes luminescence can be recorded.[135] Therefore, investigation and visualization is possible for deeper-lying tissues (biological tissues are more transparent in the IR range than in the visible or UV range) and a better signal-to-noise ratio can be achieved even against the self-luminescence of biological tissues.

The morphology of structures combining magnetic and luminescent nanoparticles with lanthanide ions can be different depending on the tasks to be solved and the chosen methods of synthesis (Fig. 26). Zhang *et al.*[157] considered multilayer structures of the core–shell type. The core was formed by Fe_2O_3 nanoparticles and the SiO_2 shell was coated by a layer of α-$NaYF_4$/Yb,Er (Fe_3O_4@SiO_2@α-$NaYF_4$/Yb,Er). Structures with the Fe_3O_4/SiO_2 core surrounded by luminescent $GdPO_4:Eu^{3+}$ nanoneedles were also proposed.[158] Yet another probable morphology is the core consisting of lanthanide-doped nanoparticles and coated with a SiO_2 shell with encapsulated magnetic nanoparticles ($NaYF_4$:Yb,Er/Tm@SiO_2@Fe_3O_4).[159] Also, structures containing luminescent components (organic dyes and nanoparticles with lanthanide ions) apart from magnetic nanoparticles can also be synthesized.[160] In this case, luminescence of both the lanthanide and the organic dye can be excited simultaneously.

III.3.c. Multifunctional HMN systems for biomedical applications

Analysis of modern publications demonstrated that development of investigations related to hybrid magnetic nanostructures is aimed at extension of their functional properties by adding more components to the system. As a rule, in these cases of HMN design, carbon nanotubes and mesoporous quartz nanoparticles are used as matrices, or so-called platforms for the deposition of functional components.[161–163] The components used as functional groups are dictated by the problem to be solved: these may be medicinal agents, biomolecules responsible for targeting or luminescent and light-sensitive components. The fabrication of HMN based on carbon nanotubes is schematically shown in Fig. 27. By using these materials, it is possible to solve sophisticated problems: manipulation *via* external magnetic field (attachment of magnetite Fe_3O_4 nanoparticles), targeting of tumour cells (*via* functionalization by folic acid), tumour cell visualization [*via* attachment of a luminescent dye — fluorescein isothiocyanate (FITC)] and delivery of the doxorubicin drug to tumour cells.[18]

Quite a number of recent publications report successful experiments dealing with the synthesis and *in vivo* applications of this type of multifuctional HMN systems to solve problems of targeted delivery, action of drugs, cancer cell visualization[164, 165] and tracing (in the case of diseases of blood-forming organs)[166, 167] and diagnosis and treatment of lymphatic system diseases.[168] In all cases, variation of components is possible: gemcitabine, camptothecin and so on as the drug; quantum dots, organic compounds and luminophores based on lanthanide ions as luminescent labels; magnetic nanoparticles (Ni, $MnFe_2O_4$, *etc.*).

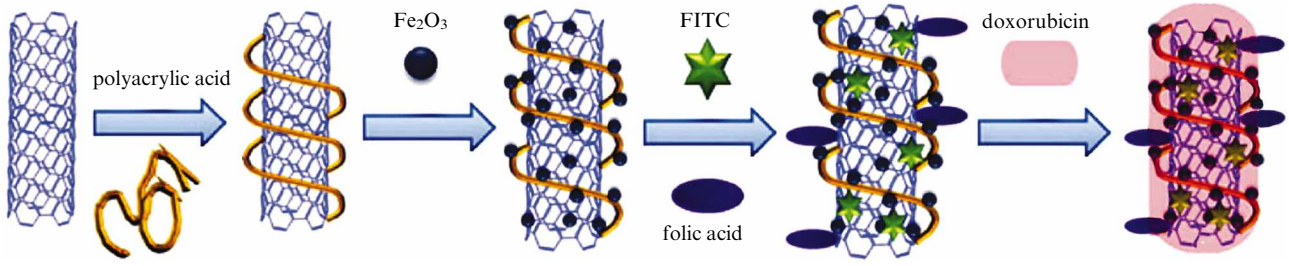


Figure 27. Scheme of the functionalization of carbon nanotubes upon attachment of magnetic nanoparticles (Fe_3O_4), the luminescent dye FITC and folic acid and the drug doxorubicin.[18]

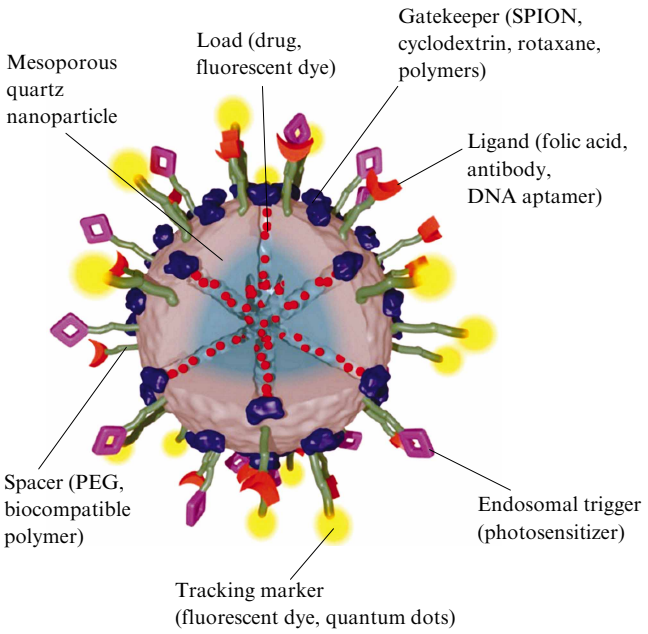


Figure 28. Multifunctional platform based on mesoporous quartz nanoparticles.[19]

The scheme illustrating the approach to the design of a multifunctional platform for the solution of the full range of biomedical problems is shown in Fig. 28.

Multifunctional platforms of this type can be based on virtually any nanostructures with a highly developed surface, for example, on mesoporous quartz nanoparticles (see Fig. 28), carbon nanotubes, graphene or polymeric and ceramic nanoparticles. It can be seen that the architecture of these particles is very complicated and implies combination of components. Depending on the tasks to be implemented, a component can be either deposited on the surface or inserted and encapsulated inside the structure. According to this approach, several medicinal agents differing in the mechanisms of action can be applied simultaneously, tissue visualization at various stages of drug action can be performed, targeted drug delivery and release can be controlled by application of a magnetic field or optical radiation.

III.3.d. Hybrid magnetic nanostructures for sorption and isolation of substances

It has been noted above that magnetic nanoparticles occurring as a part of hybrid structures enable manipulating the structures by applying an external magnetic field. This can serve for separation of substances. Among the hybrid nanomaterials combining magnetic and sorption properties, note single- or multi-walled carbon nanotubes with encapsulated magnetic nanoparticles (of magnetite or maghemite) and systems based on graphene oxide and double metal hydroxides.[169,170] The greatest number of publications devoted to sorption and impurity isolation using HMN consider carbon nanotubes with magnetic nanoparticles. The possibility of using these structures for subsoil water treatment to remove toxic impurities such as arsenic is being discussed; these structures can also be demanded for biomedical applications, in particular, for detection of traces of various types of antibiotics (in particular, fluoroquinolones and quinolones) in complex bioorganic media, for example, in blood plasma.[170]

Yang *et al.*[171] considered a more complicated HMN system, which demonstrated an exceptionally high performance in the extraction of organic dyes (*e.g.*, methyl orange) from aqueous solutions. Double metal hydroxides $[M^{2+}_{1-x}M^{3+}_{x}(OH)_2][An^-]_{x/n}\cdot y\,H_2O$ (M^{2+}, M^{3+} are doubly and triply charged metal cations) were used as the sorption agents, the unique sorption properties of which are due to the layered structure.[172,173] Another constituent of this HMN system is graphene oxide functioning as the matrix for the magnetic and sorption components. Furthermore, graphene oxide has sorption properties due to the extensive surface and the oxygen functional groups present on the surface. Thus, combining graphene oxide and layered double hydroxides in one structure provides effective sorption of organic dyes from solutions. The structure contains a magnetic component (for example, nickel nanoparticles); therefore, HMN together with the sorbed substance can be removed from solution by applying an external magnetic field. Also, the possibility of regeneration and reuse of the proposed HMN structures was demonstrated.

III.3.e. Hybrid magnetic nanomaterials for recoverable catalysts

Yet another line of research that was stimulated by nanotechnologies is the development of new types of high performance catalysts for a broad range of chemical reactions. The use of nanocatalysts can ensure, first, high

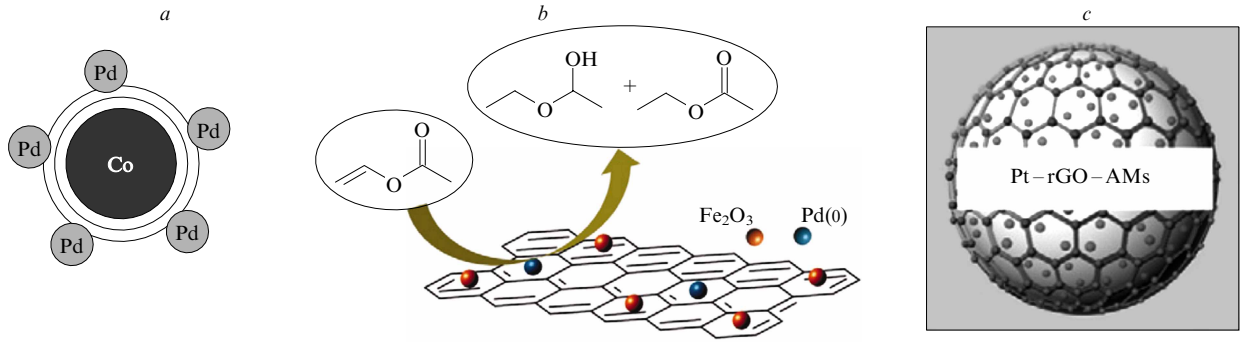


Figure 29. Catalytically active HMN systems of different morphology.
(*a*) Core–shell,[177] (*b*) nanoparticles on the graphene surface,[174] (*c*) Pt–rGO–AMs system — platinum nanoparticles on the surface of the reduced graphene oxide (rGO) sphere functionalized by amino groups (AMs) and magnetic Fe_3O_4 nanospheres.[175]

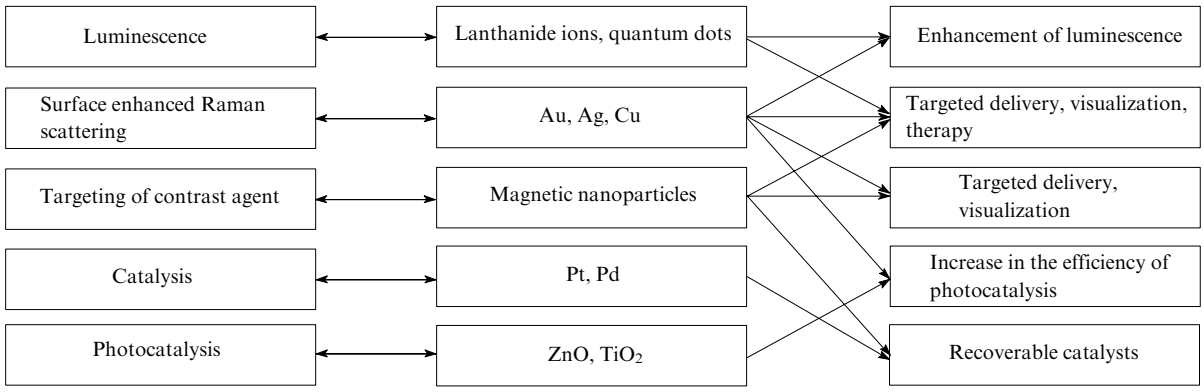


Figure 30. Diagram demonstrating the properties of hybrid nanomaterials.

activity and selectivity characteristic of homogeneous catalytic systems and, second, the possibility of recovery and reuse, as in the case of heterogeneous catalysts. The recovery and reuse of catalysts is possible for complex HMN systems owing to the possibility of separation in a magnetic field. The development of recoverable nanocatalysts is of interest from not only economical but also environmental standpoint to develop green chemistry processes.

The catalytically active HMN systems are multicomponent structures comprising magnetic nanoparticles, nanoparticles of the catalysts (most often, transition metals) and the supporting matrix (graphene, mesoporous carbon, SiO_2, *etc*.). The architecture of these structures can be different [174–177] ranging from single- or multi-layer carbon structures to multilayer core–shell systems (Fig. 29).

However, according to investigations, single- or multilayer carbon structures are less efficient than the core–shell systems because layers stick together, which leads to the loss of the functional properties of the internal areas.[175, 176] To date, the efficiency and the possibility of recovery and reuse of HMN-based catalytic systems were demonstrated for a number of reactions including alkene hydrogenation, Heck and Suzuki cross-couplings and oxidation of alcohols including methanol.[175, 177–179]

IV. Conclusion

The successful development of methods for the synthesis of various nanostructures with controlled parameters such as the composition, size and morphology paved the way to the development of more complex structures — hybrid nanomaterials. The diversity of modern methods for the synthesis of such hybrid materials allows the fabrication of very intricate structures of virtually any morphology, the properties being determined by the constituents. Two-component systems may be luminescent and magnetic, luminescent and plasmonic, magnetic and plasmonic, and magnetic and catalytic. The increase in the number of constituents extends the functional properties of the material. The diagram demonstrating extension of the properties of nanostructures *via* aggregation and formation of hybrid materials is presented in Fig. 30.

Thus, to endow the hybrid materials with specified functional properties, it is necessary to introduce the appropriate set of components into the structure. The key requirements to the size and morphology of components of hybrid nanomaterials are dictated, first of all, by the functional properties of the nanomaterials; as a rule, it is necessary to use nanostructures of small size (from several to several tens of nanometres) with a narrow size distribution. The modern trends in the development and manufacture of hybrid materials are mainly based on the matrix approach, which implies the use of so-called platforms for the deposition/insertion of functional components. As these platforms, structures with a large surface area are used such as carbon nanotubes, mesoporous quartz nanoparticles, graphene and polymeric or ceramic nanoparticles. It is noteworthy that the platform is often an active rather than inert component of the hybrid material, which provides, for example, sorption properties.

Further research into the development and investigation of hybrid nanomaterials would be aimed, in all probability, at the synthesis of more intricate structures (*e.g*., nanostars or nanoflowers),[180–182] which have exceptionally large surface area and, hence, would ensure marked enhancement of functional properties compared with the properties of hybrid materials of the same composition but simpler morphology. These structures are also of interest for fundamental science, because studying them would make it possible to follow the change in the physicochemical properties and electronic structure upon the change in the size and shape.

This review was prepared with the financial support of the Ministry of Education and Science of the Russian Federation in terms of the Agreement No. 14.604.21.0078 (unique identification number RFMEFI 60414X0078).

References

1. X Meng, K Fujita, Y Moriguchi, Y Zong, K Tanaka *Adv. Opt. Mater*. **1** 573 (2013)
2. L Zhang, D A Blom, H Wang *Chem. Mater*. **23** 4587 (2011)
3. D Mongin, V Juvé, P Maioli, A Crut, N D Fatti, F Vallee *Nano Lett*. **11** 3016 (2011)
4. J Yang, F Zhang, Y Chen, S Qian, P Hu, W Li, Y Deng, Y Fang, L Han, M Luqman, D Zhao *Chem. Commun*. **47** 11618 (2011)
5. X Sun, Y Li *Langmuir* **21** 6019 (2005)
6. T Wei, C Q Jin, W Zhong, J-M Liu *Appl. Phys. Lett*. **91** 222907 (2007)
7. G Menagen, J E Macdonald, Y Shemesh, I Popov, U Banin *J. Am. Chem. Soc*. **131** 17406 (2009)

8. E Shaviv, O Schubert, M-A Santos, G Goldoni, R D Felice, F Vallee *ACS Nano* **5** 4712 (2011)
9. G A Sotiriou, A M Hirt, P-Y Lozach, A Teleki, F Krumeich, S E Pratsinis *Chem. Mater.* **23** 1985 (2011)
10. J T Bahns, S K R S Sankaranarayanan, S K Gray, L Chen *Phys. Rev. Lett.* **106** 095501 (2011)
11. S J Henley, P C P Watts, N Mureau, S Ravi, P Silva *Appl. Phys. A* **93** 875 (2008)
12. A A Manshina, A V Povolotskiy, A V Povolotskaya, T Yu Ivanova, I O Koshevoy, S P Tunik, M Suvanto, T A Pakkanen *Surf. Coat. Technol.* **206** 3454 (2012)
13. A Povolotskiy, A Povolotckaia, Y Petrov, A Manshina, S Tunik *Appl. Phys. Lett.* **103** 113102 (2013)
14. X Wang, X Li, D Liu, Sh Song, H Zhang *Chem. Commun.* **48** 2885 (2012)
15. S Narayanan, B N Sathy, U Mony, M Koyakutty, S V Nair, D Menon *ACS Appl. Mater. Interfaces* **4** 251 (2012)
16. H Genuino, H Huang, E Njagi, L Stafford, S L Suib, in *Handbook of Green Chemistry. Green Nanoscience* (Eds A Perosa, M Selvav) (Weinheim: Wiley-VCH, 2012) Vol. 8, p. 217
17. A Shen, L Chen, W Xie, J Hu, A Zeng, R Richards, J Hu *Adv. Funct. Mater.* **20** 969 (2010)
18. Y J Lu, K C Wei, C C Ma, S Y Yang, J P Chen *Colloids Surf., B* **89** 1 (2012)
19. C Argyo, V Weiss, C Braeuchle, T Bein *Chem. Mater.* **26** 435 (2014)
20. L Carbone, P D Cozzoli *Nano Today* **5** 449 (2010)
21. R Costi, A E Saunders, U Banin *Angew. Chem., Int. Ed.* **49** 4878 (2010)
22. L A Chernozatonsky, P B Sorokin, A A Artukh *Russ. Chem. Rev.* **83** 251 (2014)
23. E G Rakov *Russ. Chem. Rev.* **82** 27 (2013)
24. V A Gerasin, E M Antipov, V V Karbushev, V G Kulichikhin, G P Karpacheva, R V Talrose, Ya V Kudryavtsev *Russ. Chem. Rev.* **82** 303 (2013)
25. S Panigrahi, S Kundu, S K Ghosh, S Nath, T Pal *J. Nanopart. Res.* **6** 411 (2004)
26. H Hei, H He, R Wang, X Liu, G Zhang *Soft Nanosci. Lett.* **2** 34 (2012)
27. R A Khaydarov, R R Khaydarov, O Gapurova, Y Estrin, Th Scheper *J. Nanopart. Res.* **11** 1193 (2009)
28. B H Kim, M J Hackett, J Park, T Hyeon *Chem. Mater.* **26** 59 (2014)
29. J Zhou, R Sedev, D Beattie, J Ralston *Langmuir* **24** 4506 (2008)
30. N Harris, M J Ford, M B Cortie, A M McDonagh *Nanotechnology* **18** 365301 (2007)
31. M J Berr, A Vaneski, C Mauser, S Fischbach, A S Susha, A L Rogach, F Juckel, J Feldmann *Small* **8** 291 (2011)
32. J Turkevich, P C Stevenson, J Hiller *Discuss. Faraday Soc.* **11** 55 (1951)
33. E Butovsky, A Irzh, B Markovsky, A Gedanken *New J. Chem.* **36** 155 (2012)
34. S J Oldenburg, R D Averitt, S L Westcott, N J Halas *Chem. Phys. Lett.* **288** 243 (1998)
35. J L Lyon, D A Fleming, M B Stone, P Schiffer, M E Williams *Nano Lett.* **4** 719 (2004)
36. X Wang, X Zhang, W Cheng, H Shao, X Liu, X Li, H Liu, J Wu *Nanoscale Res. Lett.* **9** 109 (2014)
37. I O Koshevoy, A J Karttunen, S P Tunik, M Haukka, S I Selivanov, A S Melnikov, P Yu Serdobintsev, T A Pakkanen *Organometallics* **28** 1369 (2009)
38. M Fan, G F S Andrade, A G Brolo *Anal. Chim. Acta* **693** 7 (2011)
39. C R Yonzon, D A Stuart, X Zhang, A D McFarland, C L Haynes, R P VanDuyne *Talanta* **67** 438 (2005)
40. J Hu, Z Wang, J Li *Sensors* **7** 3299 (2007)
41. C Yuen, W Zheng, Z Huang, J Innov *Opt. Heal. Sci.* **1** 267 (2008)
42. Š Bálint, S Rao, M Sánchez, V Huntošová, P Miškovský, D Petrov *J. Biomed. Opt.* **15** 027005 (2010)
43. J Evan, L Ru, C Eric, P G Etchegoin *J. Am. Chem. Soc.* **134** 14466 (2009)
44. J Evan, L Ru, C Eric, M Matthias, P G Etchegoin *J. Phys. Chem. C* **111** 13794 (2007)
45. S Nie, S R Emory *Science* **275** 1102 (1997)
46. B Sharma, R R Frontiera, A-I Henry, E Ringe, R P Van Duyne *Mater. Today* **15** 16 (2012)
47. D D Evanoff, J G Chumanov *Chem. Phys. Chem.* **6** 1221 (2005)
48. D Werner, S Hashimoto, T Tomita, S Matsuo, Y Makita *J. Phys. Chem. C* **112** 16801 (2008)
49. E Caballero-Díaz, C Pfeiffer, L Kastl, P Rivera-Gil, B Simonet, M Valcvrcel, J Jiménez-Lamana, F Laborda, W J Parak *Part. Part. Syst. Charact.* **30** 1079 (2013)
50. J J Feng, U Gernert, P Hildebrandt, I M Weidinger *Adv. Funct. Mater.* **20** 1954 (2010)
51. F X Liu, Z S Cao, C J Tang, L Chen, Z L Wang *ACS Nano* **4** 2643 (2010)
52. L Bao, S M Mahurin, S Dai *Anal. Chem.* **76** 4531 (2004)
53. Y K Kim, S W Han, D H Min *ACS Appl. Mater. Interfaces* **4** 6545 (2012)
54. A A Farah, R A Alvarez-Puebla, H Fenniri *J. Colloid Interface Sci.* **319** 572 (2008)
55. S Porel, N Venkatram, D N Rao, T P Radhakrishnan *J. Nanosci. Nanotechnol.* **7** 1887 (2007)
56. S Fateixa, A V Girao, H I S Nogueira, T Trindade *J. Mater. Chem.* **21** 15629 (2011)
57. J F Li, Y F Huang, Y Ding, S B Li, Z L Yang, X S Zhou, F R Fan, W Zhang, Z Y Zhou, D Y Wu, B Ren, Z L Wang, Z Q Tian *Nature (London)* **18** 352 (2010)
58. A Dandapat, S Pramanik, S Bysakh, G De *J. Nanopart. Res.* **15** 1804 (2013)
59. Y Q Wang, S Ma, Q Q Yang, X J Li *Appl. Surf. Sci.* **258** 5881 (2012)
60. Y F Chan, C X Zhang, Z L Wu, D M Zhao, W Wang *Appl. Phys. Lett.* **102** 183188 (2013)
61. G M Herrera, A C Padilla, S P Hernandez-Rivera *Nanomaterials* **3** 158 (2013)
62. S Hong, X Li *J. Nanomater.* Art. No 79323 (2013)
63. T Tan, C Tian, Z Ren, J Yang, Y Chen, L Sun, Z Li, A Wu, J Yin, H Fu *Phys. Chem. Chem. Phys.* **15** 21034 (2013)
64. Y Nishijima, S Akiyama *Opt. Mater. Express.* **2** 1226 (2012)
65. Y Herbani, T Nakamura, S Sato *J. Phys. Chem. C* **115** 21592 (2011)
66. F Hajiesmaeilbaigi, A Motamedi *Laser Phys.* **4** 133 (2007)
67. M S Shore, J Wang, A C Johnston-Peck, A L Oldenburg, J B Tracy *Small* **7** 230 (2011)
68. M A Garcia *J. Phys. D: Appl. Phys.* **44** 283001 (2011)
69. S Besner, M Meunier *J. Phys. Chem. C* **114** 10403 (2010)
70. D-H Chen, C-J Chen *J. Mater. Chem.* **12** 1557 (2002)
71. A N Sidorov, G W Sawinski, A H Jayatissa, F P Zamborini, G U Sumanasekera *Carbon* **50** 699 (2012)
72. A N Sreekumaran, R T Tom, V R R Kumar, C Subramaniam, T Pradeep *COSMOS* **3** 103 (2007)
73. D A Zherebtsova, D M Galimova, A V Lashkulb, V V D'yachuka, E Lyakhderantab, G G Mikhailova, I Ojalac, R Laiho *Inorg. Mater.: Appl. Res.* **2** 524 (2011)
74. H Kang, J Yim, S Jeong , J-K Yang, S Kyeong, S-J Jeon, J Kim, K D Eom, H Lee, H-I Kim, D H Jeong, J-H Kim, Y-S Lee *ACS Appl. Mater. Interfaces* **5** 12804 (2013)
75. H-Y Wu, B T Cunningham *Appl. Phys. Lett.* **98** 153103 (2011)
76. H Ko, S Chang, V V Tsukruk *ACS Nano* **3** 181 (2009)
77. Y Zang, J Yin, X He, C Yue, Z Wu, J Li, J Kang *J. Mater. Chem. A* **2** 7747 (2014)
78. K Yee *IEEE Transact. Antenn. Prop.* **14** 302 (1966)
79. H Weia, H Xu *Nanoscale* **5** 10794 (2013)

80. L Li, T Hutter, U Steinerc, S Mahajan *Analyst* **138** 4574 (2013)
81. K Kneipp, H Kneipp *Appl. Spectrosc.* **60** 12 (2006)
82. K Kneipp, Y Wang, H Kneipp, L T Perelman, I Itzkan, R R Dasari, M S Feld *Phys. Rev. Lett.* **78** 1667 (1997)
83. M Mahanti, D Basak *J. Lumin.* **145** 19 (2014)
84. Y Wang, J Tang, L Huang, Y Wang, Z Huang, J Liu, Q Xu, W Shen, L A Belfiroe *Opt. Mater.* **35** 1395 (2013)
85. G An, C Yang, Y Zhou, X Zhao *Phys. Status Solidi, A* **209** 2583 (2012)
86. B-T Liu, T-H Liao, S Tseng, M-H Lee *Appl. Surf. Sci.* **292** 615 (2014)
87. N Niu, F He, P Ma, S Gai, G Yang, F Qu, Y Wang, J Xu, P Yang *ACS Appl. Mater. Interfaces* **6** 3250 (2014)
88. S Jayaraman, P S Kumar, D Mangalaraj, D Rajarathnam, S Ramakrishna, M P Srinivasan *RSC Adv.* **4** 11288 (2014)
89. P Wu, T Zhao, Y Tian, L Wu, X Hou *Chem. – Eur. J.* **19** 7473 (2013)
90. G Das, R Chakraborty, A Gopalakrishnan, D Baranov, E D Fabrizio, R Krahne *J. Nanopart. Res.* **15** 1596 (2013)
91. W Xu, X Min, X Chen, Y Zhu, P Zhou, S Cui, S Xu, L Tao, H Song *Sci. Rep.* **4** 5087 (2014)
92. P Zhao, Y Zhu, X Yang, K Fan, J Shen, C Li *RSC Adv.* **2** 10592 (2012)
93. F Auzel *Chem. Rev.* **104** 139 (2004)
94. L Esterowitz, J Noonan, J Bahler *Appl. Phys. Lett.* **10** 126 (1967)
95. A Rapaport, J Milliez, M Bass, L Fellow, A Cassanho *J. Disp. Technol.* **2** 68 (2006)
96. X Yu, M Li, M Xie, L Chen, Y Li, Q Wang *Nano Res.* **3** 51 (2010)
97. L Wang, R Yan, Z Huo, L Wang, J Zeng, J Bao, X Wang, Q Peng, Y Li *Angew. Chem., Int. Ed.* **44** 6054 (2005)
98. F Wang, X G Liu *Chem. Soc. Rev.* **38** 976 (2009)
99. Q F Zhang, C S Dandeneau, X Y Zhou, G Z Cao *Adv. Mater.* **21** 4087 (2009)
100. H Zhu, C X Shan, L K Wang, Y Yang, J Y Zhang, B Yao, D Z Shen, X W Fan *Appl. Phys. Lett.* **96** 041110 (2010)
101. R F Oulton, V J Sorger, T Zentgraf, R M Ma, C Gladden, L Dai, G Bartal, X Zhang *Nature (London)* **461** 629 (2009)
102. C Soci, A Zhang, B Xiang, S A Dayeh, D P R Aplin, J Park, X Y Bao, Y H Lo, D Wang *Nano Lett.* **7** 1003 (2007)
103. J S Liu, C X Shan, B H Li, Z Z Zhang, C L Yang, D Z Shen, X W Fan *Appl. Phys. Lett.* **97** 251102 (2010)
104. M S Zhu, P L Chen, M H Liu *ACS Nano* **5** 4529 (2011)
105. F Zhao, X Li, J Zheng, X Jang *Chem. Mater.* **20** 1197 (2008)
106. S Sarkar, D Basak *Sens. Actuators B* **176** 374 (2013)
107. D M Bagnal, Y F Chen, Z Zhu, T Yao *Appl. Phys. Lett.* **73** 1038 (1998)
108. Y J Fang, J Sha, Z L Wang, Y T Wan, W W Xia, Y W Wang *Appl. Phys. Lett.* **98** 033103 (2011)
109. N R Yogamalar, A C Bose *J. Alloys Compd.* **509** 8493 (2011)
110. X Y Xue, Z H Chen, L L Xing, C H Ma, Y J Chen, T H Wang *J. Phys. Chem. C* **114** 18607 (2010)
111. J M Lin, H Y Lin, C L Cheng, Y F Chen *Nanotechnology* **17** 4391 (2006)
112. C W Cheng, E J Sie, B Liu, C H A Huan, T C Sum, H D Sun, H J Fan *Appl. Phys. Lett.* **96** 071107 (2010)
113. M K Lee, T G Kim, W Kim, Y M Sung *J. Phys. Chem. C* **112** 10079 (2008)
114. X H Li, Y Zhang, X J Ren *Opt. Express* **17** 8735 (2009)
115. V Subramanian, E E Wolf, P V Kamat *J. Phys. Chem. B* **107** 7479 (2003)
116. Y K Mishra, S Mohapatra, R Singhal, D K Avasthi, D C Agarwal, S B Ogale *Appl. Phys. Lett.* **92** 043107 (2008)
117. M Mahanti, T Ghosh, D Basak *Nanoscale* **3** 4427 (2011)
118. J Song, X Y An, J Y Zhou, Y X Liu, W Wang, X D Li, W Lan, E Q Xie *Appl. Phys. Lett.* **97** 122103 (2010)
119. W Z Liu, H Y Xu, C L Wang, L X Zhang, C Zhang, S Y Sun, J G Ma, X T Zhang, J N Wang, Y C Liu *Nanoscale* **5** 8634 (2013)
120. H Shen, C X Shan, Q Qiao, J S Liu, B H Li, D Z Shen *J. Mater. Chem. C* **1** 234 (2013)
121. X L Li, H L Hu, D H Li, Z X Shen, Q H Xiong, S Z Li, H J Fan *ACS Appl. Mater. Interfaces* **4** 2180 (2012)
122. X X Zou, R Silva, X X Huang, J F Al-Sharab, T Asefa *Chem. Commun.* **49** 382 (2013)
123. G Sinha, L E Depero, I Alessandri *ACS Appl. Mater. Interfaces* **3** 2557 (2011)
124. A Ramakrishnan, S Neubert, B Mei, J Strunk, L D Wang, M Bledowski, M Muhler, R Beranek *Chem. Commun.* **48** 8556 (2012)
125. X H Li, G Y Chen, L B Yang, Z Jin, J H Liu *Adv. Funct. Mater.* **20** 2815 (2010)
126. Z W Seh, S H Liu, M Low, S Y Zhang, Z L Liu, A Mlayah, M Y Han *Adv. Mater.* **24** 2310 (2012)
127. A Mclaren, T Valdes-Solis, G Q Li, S C Tsang *J. Am. Chem. Soc.* **131** 12540 (2009)
128. A B F Martinson, J W Elam, J T Hupp, M J Pellin *Nano Lett.* **7** 2183 (2007)
129. J C Bernede, Y Berredjem, L Cattin, M Morsli *Appl. Phys. Lett.* **92** 083304 (2008)
130. M D Xiao, R B Jiang, F Wang, C H Fang, J F Wang, J C Yu *J. Mater. Chem. A* **1** 5790 (2013)
131. S Linic, P Christopher, D B Ingram *Nat. Mater.* **10** 911 (2011)
132. K Awazu, M Fujimaki, C Rockstuhl, J Tominaga, H Murakami, Y Ohki, N Yoshida, T Watanabe *J. Am. Chem. Soc.* **130** 1676 (2008)
133. S C Thimsen, E Warren *Energy Environ. Sci.* **5** 5133 (2012)
134. S Tang, S Vongehr, G He, L Chen, X Meng *J. Colloid Interface Sci.* **375** 125 (2012)
135. Y Hu, H Zhang, P Wu, H Zhang, B Zhou, C Cai *Phys. Chem. Chem. Phys.* **13** 4083 (2011)
136. J Liu, H Q Yang, F Kleitz, Z G Chen, T Yang, E Strounina, G Q Lu, S Z Qiao *Adv. Funct. Mater.* **22** 591 (2012)
137. S P Gubin, Yu A Koksharov, G B Khomutov, G Yu Yurkov *Russ. Chem. Rev.* **74** 489 (2005)
138. A G Pershina, A E Sazonov, V D Filimonov *Russ. Chem. Rev.* **83** 299 (2014)
139. H W Yang, M-Y Hua, H-L Liu, C-Y Huang, K-C Wei *Nanotechnol. Sci. Appl.* **5** 73 (2012)
140. A S Hoffman *J. Control. Rel.* **132** 153 (2008)
141. K Iwai, H Maeda, T Konno *Cancer Res.* **44** 2115 (1984)
142. J Chomoucka, J Drbohlavova, D Huska, V Adam, R Kizek, J Hubalek *Pharmacol. Res.* **62** 144 (2010)
143. I Robinson, L D Tung, S Maenosono, C Walti, N T K Thanh *Nanoscale* **2** 2624 (2010)
144. M Guo, C Que, C Wang, X Liu, H Yan, K Liu *Biomaterials* **32** 185 (2011)
145. R J Holmberg, A-J Hutchings, F Habib, I Korobkov, J C Scaiano, M Murugesu *Inorg. Chem.* **52** 14411 (2013)
146. H Yan, M Guo, K Liu, in *Biomedical Science, Engineering and Technology: Multifunctional Magnetic Hybrid Nanoparticles as a Nanomedical Platform for Cancer-Targeted Imagine and Therapy*. (Ed. D N Ghista) (InTech, 2012) Ch. 12, p. 902
147. X Yang, X Zhang, Y Ma, Y Huang, Y Wanga, Y Chen *J. Mater. Chem.* **19** 2710 (2009)
148. C Gao, W Li, H Morimoto, Y Nagaoka, T Maekawa *J. Phys. Chem. B* **110** 7213 (2006)
149. G Korneva, H Ye, Y Gogotsi, D Halverson, G Friedman, J C Bradley, K G Kornev *Nano Lett.* **5** 879 (2005)
150. C Muller, A Leonhardt, M C Kutz, B Buchner, H Reuther *J. Phys. Chem. C* **113** 2736 (2009)
151. E C Vermisoglou, G Pilatos, G E Romanos, E Devlin, N K Kanellopoulos, G N Karanikolos *Nanotechnology* **22** 355602 (2011)

152. H-M Fan, M Olivo, B Shuter, J-B Yi, R Bhuvaneswari, H-R Tan, G-C Xing, C-T Ng, L Liu, S S Lucky, B-H Bay, J Ding *J. Am. Chem. Soc.* **132** 14803 (2010)
153. Z Wang, L Wu, M Chen, S Zhou *J. Am. Chem. Soc.* **131** 11276 (2009)
154. G Ruan, D Thakur, S Deng, S Hawkins, J O Winter *Proceedings of the Institution of Mechanical Engineers, Part N: J. Nanoeng. Nanosyst.* **223** 81 (2009)
155. T A Larson, J Bankson, J Aaron, K Sokolov *Nanotechnology* **18** 325101 (2007)
156. X Li, D Zhao, F Zhang *Theranostics* **3** 292 (2013)
157. F Zhang, G B Braun, A Pallaoro, Y Zhang, Y Shi, D Cui, M Moskovits, D Zhao, G D Stucky *Nano Lett.* **12** 61 (2012)
158. M Runowski, T Grzyb, S Lis *J. Nanopart. Res.* **14** 1188 (2012)
159. D Hu, M Chen, Y Gao, F Li, L Wu *J. Mater. Chem.* **21** 11276 (2011)
160. H Xu, L Cheng, C Wang, X Ma, Y Li, Z Liu *Biomaterials* **32** 9364 (2011)
161. V Cauda, H Engelke, A Sauer, D Arcidet, C Brauchle, J Radler, T Bein *Nano Lett.* **10** 2484 (2010)
162. B Chang, J Guo, C Liu, J Qian, W Yang *J. Mater. Chem.* **20** 9941 (2010)
163. Á Muñoz-Noval, V Sánchez-Vaquero, V Torres-Costa, D Gallach, M Manso-Silván, J P García-Ruiz, M Hernando-Pérez, P J de Pablo, R J Martín-Palma *J. Nanophoton.* **5** 051505 (2011)
164. J J Khandare, A Jalota-Badhwar, S D Satavalekar, S G Bhansali, N D Aher, F Kharas, S S Banerjee *Nanoscale* **4** 837 (2012)
165. M L Chen, Y J He, X W Chen, J H Wang *Langmuir* **28** 16469 (2012)
166. H Gul, W Lu, P Xu, J Xing, J Chen *Nanotechnology* **21** 155101 (2010)
167. D Cai, J M Mataraza, Z H Qin, Z Huang, J Huang, T C Chiles, D Carnahan, K Kempa, Z Ren *Nat. Methods* **2** 449 (2005)
168. F Yang, C Jin, D Yang, Y Jiang, J Li, Y Di, J Hu, C Wang, Q Ni, D Fu *Eur. J. Cancer* **47** 1873 (2011)
169. M A Bavio, A G Lista *Sci. World J.* **2013** 1 (2013)
170. G Morales-Cid, A Fekete, B M Simonet, R Lehmann, S Cárdenas, X Zhang, M Valcárcel, P Schmitt-Kopplin *Anal. Chem.* **82** 2743 (2010)
171. Z Yang, S Ji, W Gao, C Zhang, L Ren, W W Tjiu, Z Zhang, J Pan, T Liu *J. Colloid Interface Sci.* **408** 25 (2013)
172. H Zaghouane-Boudiaf, M Boutahala, L Arab *Chem. Eng. J.* **187** 142 (2012)
173. T P F Teixeira, S I Pereira, S F Aquino, A Dias *Environ. Eng. Sci.* **29** 685 (2012)
174. S Chandra, S Bag, P Das, D Bhattacharya, P Pramanik *Chem. Phys. Lett.* **519 – 520** 59 (2012)
175. S Lin, C Shen, D Lu, C Wang, H-J Gao *Carbon* **53** 112 (2013)
176. M Zhu, G Diao *J. Phys. Chem. C* **115** 24743 (2011)
177. Q M Kainz, R Linhardt, R N Grass, G Vilé, J Pérez-Ramírez, W J Stark, O Reiser *Adv. Funct. Mater.* **24** 2020 (2014)
178. Q Du, W Zhang, H Ma, J Zheng, B Zhou, Y Li *Tetrahedron* **68** 3577 (2012)
179. M B Gawande, A Rathi, I D Nogueira, C A A Ghumman, N Bundaleski, O M N D Teodoro, P S Branco *ChemPlusChem* **77** 865 (2012)
180. P R Sajanlal, Th Pradeep *Nano Res.* **2** 306 (2009)
181. J Ge, J Lei, R N Zare *Nat. Nanotechnol.* **7** 428 (2012)
182. Q Jiang, Z Jiang, L Zhang, H Lin, N Yang, H Li, D Liu, Z Xie, Z Tian *Nano Res.* **4** 612 (2011)